Helium bubbling in a Molten Salt Fast Reactor

A flotation process

Dirkjan Journée

Master of Science Thesis

Delft, Januari 2014

Supervisors:	dr. ir. J.L. Kloosterman	TNW, TU Delft
	prof. dr. R. Konings	TNW, TU Delft
Committee:	prof. dr. R. Konings	TNW, TU Delft
	dr. ir. J.R. van Ommen	TNW, TU Delft
	dr. ir. M. Rohde	TNW, TU Delft

Delft University of Technology
Faculty of Applied Sciences
Dept. of Radiation Science & Technology
Nuclear Energy and Radiation Applications

Abstract

The Molten Salt Reactor (MSR) is one of the Generation IV nuclear reactor concepts. The molten salt reactor uses a liquid fuel, which gives the possibility to reprocess the fuel while operating the reactor. Reprocessing the fuel during operation strongly decreases the radiotoxicity of the waste and optimizes the use of natural resources.

The first part of this thesis is to examine the reprocessing steps in a Molten Salt Reactor. There are five reprocessing steps, which can be divided in on-line and off-line reprocessing. Helium bubbling is used as the on-line reprocessing technique. Fluorination, protactinium removal, actinide extraction and lanthanide extraction are used as the off-line reprocessing techniques.
It was found that the reprocessing steps show a promising molten salt reactor concept, but the individual techniques are still to be optimized. And the different steps in the reprocessing of the salt must still be connected together to form a continuous process. It was also found that the helium bubbling technique, which was initially used to extract the gaseous fission products, also extracted a part of the noble and semi-noble metals from the molten salt. These metals will not dissolve in the salt and plate out on metal surfaces in the reactor. If the plate-out is excessive, the decay heat from the noble and semi-noble metals may damage the reactor. The extraction of these metals with helium is proposed to be achieved by a flotation process. The factors that play a role in a flotation process are described by Schulze [Schulze, 1984] and Nguyen [Nguyen, 2004].

The second part and final goal of this thesis was to develop an experimental method to determine the influence of the bubble size and gas flow in a flotation process. A flotation process is described as an extraction of solids from a liquid with gas bubbles. The bubble size and gas flow are the variables that are adjustable in the helium bubbling technique in a Molten Salt Reactor. The development of this experimental method included the making of a new set-up with a newly fabricated piece of equipment and developing a method to work with this set-up.
The result of the set-up is a modified version of a Hallimond tube. The set-up is built to use the methods to examine a flotation process, which are described by Nguyen [Nguyen, 2004]. The methods are a direct and an indirect. The indirect method is based on the extraction of a known amount of particles that are added to the set-up. The direct method is filming the direct interaction of solids with gas bubbles and is used to get a better understanding of how the process works. It was found that the developed set-up is able to get good results for the direct method and promising results for the indirect method. This new equipment and the new experimental method offer the possibility for a number of follow-up studies on the topic of a flotation process.

Contents

1 Introduction

The Molten Salt Reactor (MSR) is one of the Generation IV nuclear reactor concepts. The molten salt reactor uses a liquid fuel, which gives the possibility to reprocess the fuel while operating the reactor. Reprocessing the fuel during operation strongly decreases the radiotoxicity of the waste and optimizes the use of natural resources. There are five reprocessing steps, which can be divided in on-line and off-line reprocessing. Helium bubbling is used as the on-line reprocessing technique. Fluorination, protactinium removal, actinide extraction and lanthanide extraction are used as the off-line reprocessing techniques.

The first part of this study is to examine the reprocessing steps in a Molten Salt Reactor, where the focus will be on the helium bubbling technique. Helium bubbling was initially used to extract the gaseous fission products, but it was found that this technique also extracted a part of the noble and semi-noble metals from the molten salt. These metals will not dissolve in the salt and plate out on metal surfaces in the reactor. If the plate-out is excessive, the decay heat from the noble and semi-noble metals may damage the reactor. Therefore it is important to extract these metals.

The extraction of these metals with helium is proposed to be achieved by a flotation process. The second part of this research is to develop an experimental method to determine the influence of the adjustable variables in a flotation process in the Molten Salt Reactor. The variables that can be adjusted are the bubble size and the gas flow.

1.1 Nuclear energy

1.1.1 Worldwide Energy demand

According to the International Energy Outlook 2013 the worlds energy consumption will grow with an estimated 56% between 2010 and 2040. Figure 1.1 shows a graph of the estimated energy consumption growth in quadrillion BTU or Quad (1 quad = 293 TWh). Most of the increase in global energy demand from 2010 to 2040 occurs among the developing nations outside the OECD (Organization for Economic Cooperation and Development), particularly China.

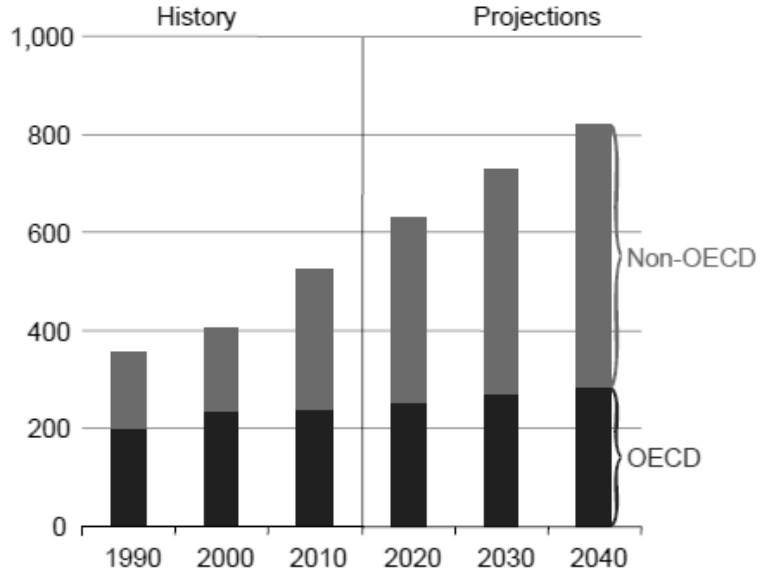

Figure 1.1 World total energy consumption, 1990-2040 (in quadrillion Btu)

There are five different fuel types for energy production:

- Petroleum and liquid fuels[1]
- Coal
- Natural gas
- Renewables (e.g. hydropower)
- Nuclear

The two fastest growing energy sources are renewables and nuclear power [IEO2013, 2013]. The impact of fossil fuel emissions on the environment and the sustained high world oil prices support the expanded use of these sources.

1.1.2 Principle of a nuclear reactor

Nuclear power is generated by a nuclear reactor and converted into electrical energy. A nuclear reactor is used to initiate and control a sustained nuclear fission reaction in order to generate electricity. A nuclear reactor is part of the nuclear fuel cycle. The nuclear fuel cycle exists of the progression of nuclear fuel through different steps. The steps can be divided into three different sections. The front end, the service period and the back end. The front end are the preparation steps of the fuel, the service period is the period where the fuel is used during reactor operation and the back end are the disposal or reprocessing steps of the spent nuclear fuel. Figure 1.2 shows an overview of the nuclear fuel cycle of uranium.

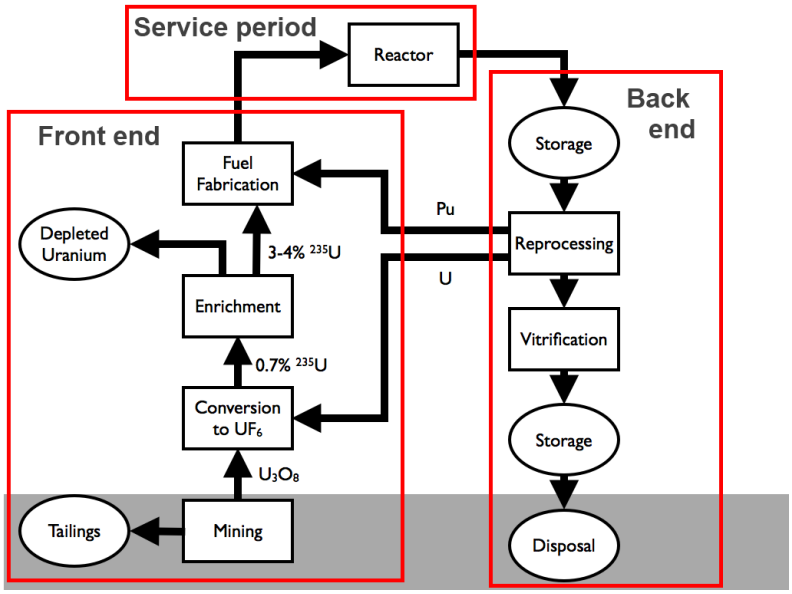

Figure 1.2. Overview of the nuclear fuel cycle of uranium.

The reactor converts the thermal energy released from nuclear fission reactions into electric energy. The conversion from thermal energy to electricity is done by steam turbines. There are a lot of different nuclear reactor designs, but the principle is: the energy from a nuclear fission reaction is used to heat a working fluid (in most cases the working fluid is water or a gas) to generate steam which runs through turbines to generate electricity. This principle design is shown in figure 1.3.

[1] In *IEO2013*, the term *petroleum and other liquid fuels* includes a full array of liquid product supplies. Petroleum liquids include crude oil and lease condensate, natural gas plant liquids, bitumen, extra-heavy oil, and refinery gains. Other liquids include gas-to-liquids, coal-to-liquids, kerogen, and biofuels.

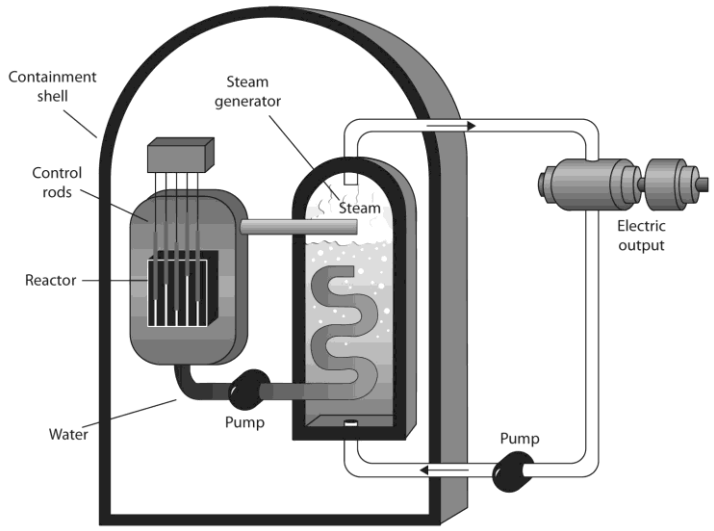

Figure 1.3. Principle of a nuclear reactor. The reactor core heats up a working fluid, in this case water, to evaporate to steam. This steam runs through a turbine to generate electricity. The steam is condensed and pumped back to the core.

The fission reactions are based on fissile materials that can sustain a chain reaction with neutrons. When a fissile nucleus absorbs a neutron, it will fission into two lighter elements (fission products) while releasing neutrons and a large amount of energy. The energy is released mainly due to the kinetic energy of the fission products and the ionizing radiation. The free neutrons can be captured by another fissile element to create a nuclear chain reaction. Figure 1.4 shows a drawing of a nuclear chain reaction.

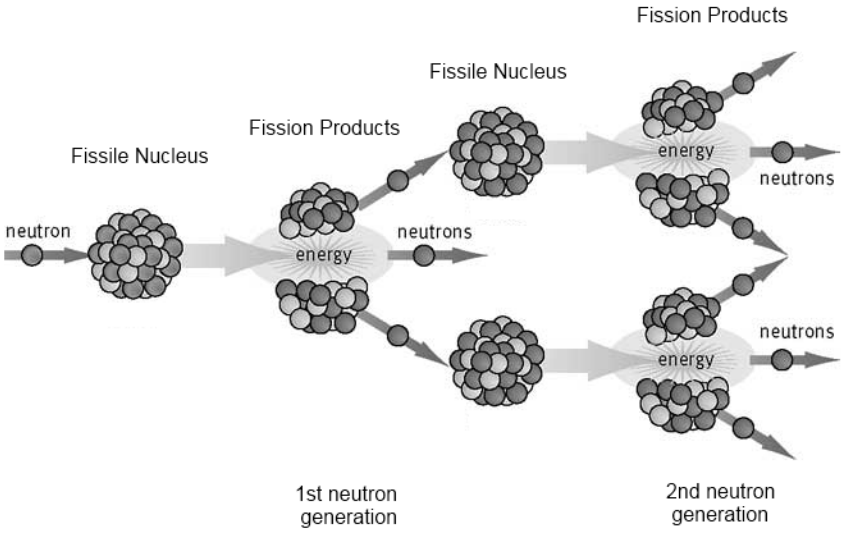

Figure 1.4. Nuclear chain reaction. A fissile nucleus captures a neutron to undergo fission while releasing energy and free neutrons.

The released neutrons have an energy of 0.7 Mev - 10 MeV, these neutrons are called fast neutrons. By means of a moderator the neutrons are slowed down till they have a velocity corresponding to the most probable energy at 20 degrees Celsius, which is about 2.2 km/s, these neutrons are called thermal neutrons and have an energy about 0.025 eV. Neutrons with different energies have different neutron absorption cross-sections, which means that the probability of an interaction with a nucleus differs.

A nuclear reactor either uses a fast neutron spectrum or a thermal neutron spectrum. The different fuels and moderators determine the neutron spectrum.

1.2 Generation IV reactors

There are a lot of different types of nuclear reactor designs. The different designs can be divided into different groups, called 'generations'. Generation I reactors are the early prototype reactors. Generation II are the first commercial reactors. Generation III reactors are the more developed Generation II reactors. The next generation reactors are the Generation IV reactors. The Generation IV International Forum (GIF) considered six different type of reactors. These reactors have to measure up to:

- reduced capital cost
- enhanced nuclear safety
- minimal generation of nuclear waste
- proliferation-resistance

The six different reactor types are summed up in table 1.1.

Table 1.1. Overview of Generation IV Reactors. [GIF, 2009]

System	***Neutron Spectrum***	***Fuel type***	***Outlet Temperature ^oC***	***Size (MWe)***
Very-high-temperature reactor (VHTR)	Thermal	Solid	900 - 1000	250 - 300
Supercritical-water-cooled reactor (SCWR)	Thermal/Fast	Solid	510 - 625	300 - 700 1000 - 1500
Gas-cooled fast reactor (GFR)	Fast	Solid	850	1200
Sodium-cooled fast reactor (SFR)	Fast	Solid	550	30 - 150 300 - 1500 1000 - 2000
Lead-cooled fast reactor (LFR)	Fast	Solid	480 - 800	20 - 180 300 - 1200 600 - 1000
Molten salt reactor (MSR)	Thermal/Fast	Liquid	700 - 800	1000

The molten salt reactor is the only design to use liquid fuel. Not only the design of a reactor can accomplish the criteria of the GIF, also the used fuel can have an influence. Uranium and plutonium are traditionally used as a fuel for nuclear reactors, but in the 1960's it was found that the thorium/uranium-233 fuel cycle can also be used for a nuclear reactor. Despite the success, the MSR program closed down in the early 1970's in favor of the liquid metal fast-breeder reactor.

1.3 Thorium fuel cycle

Thorium is the again discovered fuel for nuclear energy. The interest in thorium as a nuclear fuel comes mainly from:

- the abundance of thorium in the earth's crust compared to uranium
- the lower levels of waste generation, especially transuranic elements like neptunium, plutonium and americium
- the excellent non-proliferation credentials

Thorium itself is not fissile, but fertile. When a fissile fuel element captures a neutron it will undergo fission, while releasing large amounts of energy. When a fertile element captures a neutron it will become a fissile element.

Natural thorium is thorium-232. Thorium-232 is transmuted into fissile uranium-233 in order to use as a nuclear fuel. The production of uranium-233 from thorium-232 can be seen as a cycle, which is called the thorium fuel cycle (see figure 1.5). The thorium/uranium nuclear reactions are the following:

1. Natural thorium-232 (Th-232) captures a neutron from a fission reaction and becomes thorium-233 (Th-233).
2. Thorium-233 (Th-233) decays with a half life of 22 minutes, to protactinium-233 (Pa-233) through β^--decay.
3. Protactinium (Pa-233) decays in 27 days to uranium-233 through β^--decay.
4. Uranium-233 (U-233) undergoes fission, while releasing energy and free neutrons. The neutrons can be used to continue the cycle.

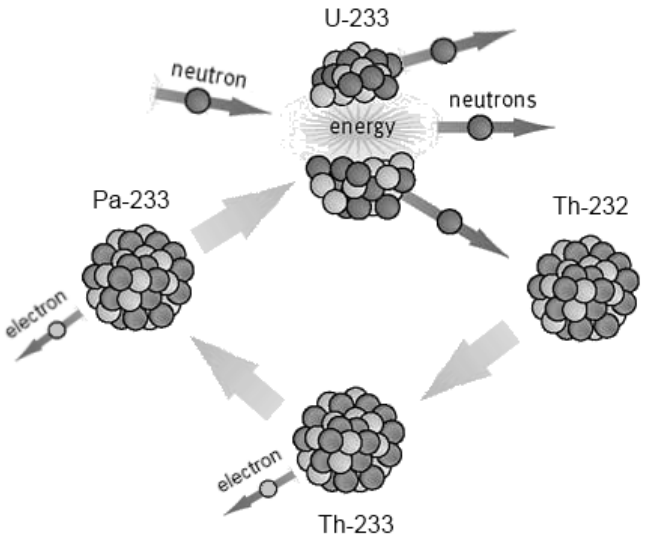

Figure 1.5. Thorium fuel cycle. Th-232 captures an neutron to Th-233. Th-233 decays to Pa-233 while releasing an electron. Pa-233 decays to fissile U-233 while releasing an electron. U-233 absorbs an neutron to undergo fission while releasing energy and free neutrons which can be captured by Th-232 to start the cycle again.

Ideally, protactinium has to be removed from the bulk to avoid the capture of a neutron. When protactinium captures a neutron, it will become non-fissile uranium-234. The breeding of uranium-233 can best be done in a molten salt reactor. The possibility of selective extraction of actinides in a

molten salt reactor makes it possible to remove the protactinium from the bulk before it can capture a neutron. This will be further explained in chapter 2.

1.4 Molten salt reactor

Nuclear reactors consist of fuel and a coolant. Most nuclear fuels contain heavy fissile elements that are capable of nuclear fission. These are solid fuels, like UOX (Uranium diOXide) or MOX (Mixed Oxide, MOX fuel consists of a mixture of plutonium and uranium), which are pressed in pellets. These pellets are sealed in fuel rods. The MSR uses a liquid fuel, in contrast to the other Generation IV reactors, which use solid fuel rods. This gives the reactor a couple of extra advantages and challenges. The MSR operates at atmospheric pressure and a temperature in the range of 625 - 775 ^{0}C. The molten salt reactor uses a liquid fuel, which gives the reactor some advantages compared to the reactors with a solid fuel [Goethem, 2008]:

- Optimum use of fissile materials
- Very low production of long-lived wastes
- Flexible waste management due to high burn-up and on-site reprocessing
- The fuel is automatically drained under accident conditions into passively cooled storage tanks
- Most gaseous fission products (krypton, xenon) are continuously removed
- No fuel fabrication is required
- Smaller equipment size because of the higher volumetric heat capacity of the salts

1.4.1 History of the molten salt reactor; ARE and MSRE

The history of the molten salt reactor starts in 1946 with the NEPA (Nuclear Energy for the Propulsion of Aircraft) project. The NEPA project worked with the ARE (Aircraft Reactor Experiment) program, which was an experiment to design a nuclear-powered bomber. The ARE was designed for operation at temperatures in the region of 1400 ^{0}C at a power of 1-3 MWth with a fluoride-salt fuel circulating in a heterogeneous core. The moderator were hot-pressed BeO blocks cooled by circulating sodium [Bettis, 1957]. The project was cancelled in 1961.

After the ARE the MSRE (Molten Salt Reactor Experiment) was started in the 1960s. The MSRE was an experimental molten salt reactor at ORNL (Oak Ridge National Laboratory) which was constructed in 1964 and went critical in 1965 until 1969. Figure 1.6 shows the MSRE.

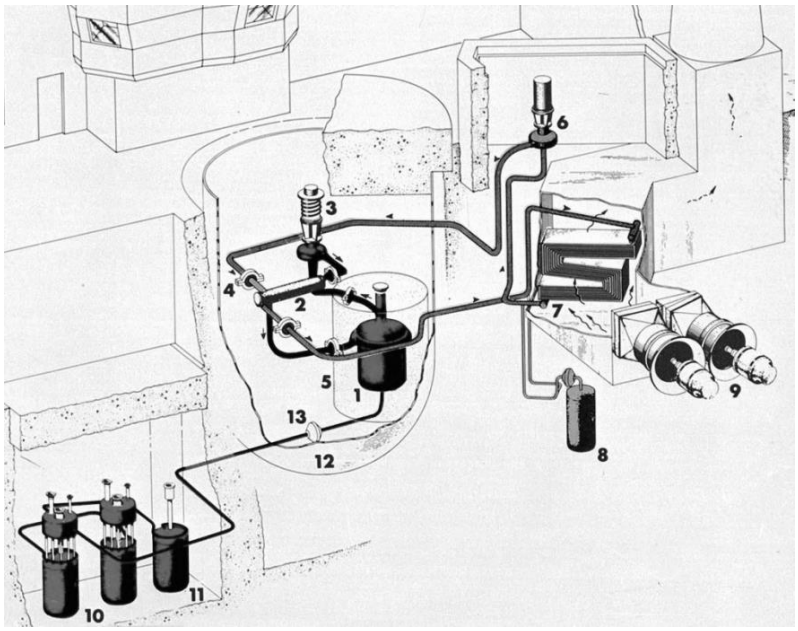

Figure 1.6. Layout of the Molten Salt Reactor Experiment. 1. Reactor vessel, 2. Heat exchanger, 3. Fuel pump, 4. Freeze flange, 5. Thermal shield, 6. Coolant pump, 7. Radiator, 8. Coolant drain tank, 9. Fans, 10. Fuel drain tank, 11. Flush tank, 12. Containment vessel, 13. Freeze valve.

The MSRE operated at 650 ^{0}C at a power of 7.4 MWt. The reactor used molten LiF-BeF_2-ZrF_4-UF_4 (65-29-5-1 mole%) as a fuel. First $^{235}UF_4$ (33% enrichment) was used. Later $^{233}UF_4$ was added to the salt, making the MSRE the first reactor to be fuelled with this fissile material [Haubenreich, 1970]. The materials for the MSRE are shown in table 1.2.

Table 1.2. Materials used in the MSRE.

Fuel salt: Composition	LiF-BeF_2-ZrF_4-UF_4 (65.0 - 29.1 - 5.0 - 0.9 mole%)
Properties at 650 ºC	
Density	2.3 g/cm^3
Specific heat	2.0 .10^3 J/kg.ºC
Thermal conductivity	1.43 W/m.ºC
Viscosity	0.008 kg/m.s
Vapour pressure	<1 .10^{-4} bar
Liquidus temperature	434 ºC
Coolant salt	LiF-BeF_2 (66-34 mole%)
Moderator	Grade CGB graphite
Salt containers	Hastelloy-N (68-Ni, 17-Mo, 7-Cr, 5-Fe)
Cover gas	Helium

During normal conditions the reactor was operating at a power of 8 MW. The inlet temperature of the fuel salt in the reactor vessel was 632 ºC and the outlet temperature was 655 ºC. The fuel salt was pumped around with a flow of 75.7 l/s. The inlet temperature of the coolant salt at the heat exchanger was 546 ºC and the outlet temperature was 579 ºC. The flow of the coolant salt was 53.6 l/s. Helium

was used as a cover gas to remove gaseous fission products like xenon and krypton. The design flow sheet is given in figure 1.7.

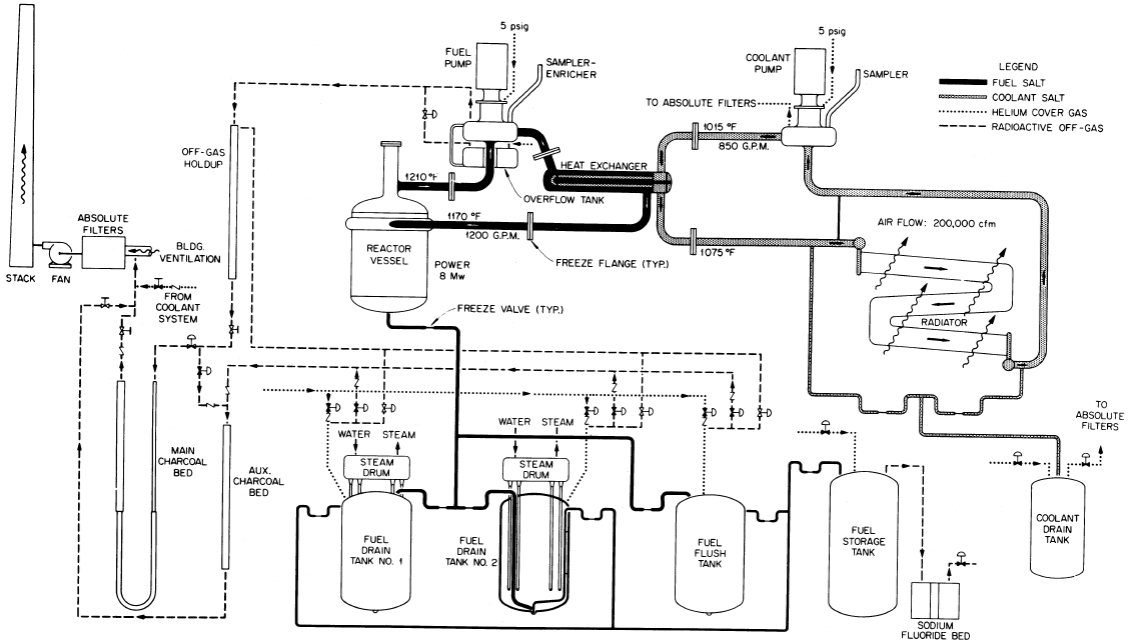

Figure 1.7. Design flow sheet of the MSRE. The reactor is operating at a power of 8 MW. The inlet temperature of the fuel salt at the reactor vessel is 632 °C (1170 °F), the outlet temperature is 655 °C (1210 °F). The flow of the fuel salt is 75.7 l/s (1200 GPM). The inlet temperature of the coolant salt at the heat exchanger is 546 °C (1015 °F) and the outlet temperature is 579 °C (1075 °F). The flow of the coolant salt is 53.6 l/s (850 GPM).

The program was terminated in the early 1970s, in favour of the Liquid metal fast-breeder reactor (LMFBR). Most of the knowledge for the newly designed molten salt reactor is based on the results from the MSRE.

1.4.2 Molten Salt Fast Reactor

The interest for the molten salt reactor resumed after the design became one of the six Generation IV reactors. There are different MSR-projects over the world. The European project is called the EVOL project (Evaluation and Viability of Liquid Fuel Fast Reactor Systems). The participants are:

- CNRS, France
- Helmoltz-Zentrum Dresden-Rossendorf, Germany
- INOPRO, France
- Joint Research Center, European Commission, Belgium
- Aubert et Duval, France
- Karlsruher Institute für Technologie, Germany
- Energovyzkum Spol S.R.O, Czech Republic
- Technische Universiteit Delft, Netherlands
- Politecnico Torino, Italy
- Budapesti Muszaki es gazdasagtudomanyi egyete, Hungary

The project is developing on the Molten Salt Fast Reactor (MSFR) concept. A schematic concept of the reactor is given in figure 1.8.

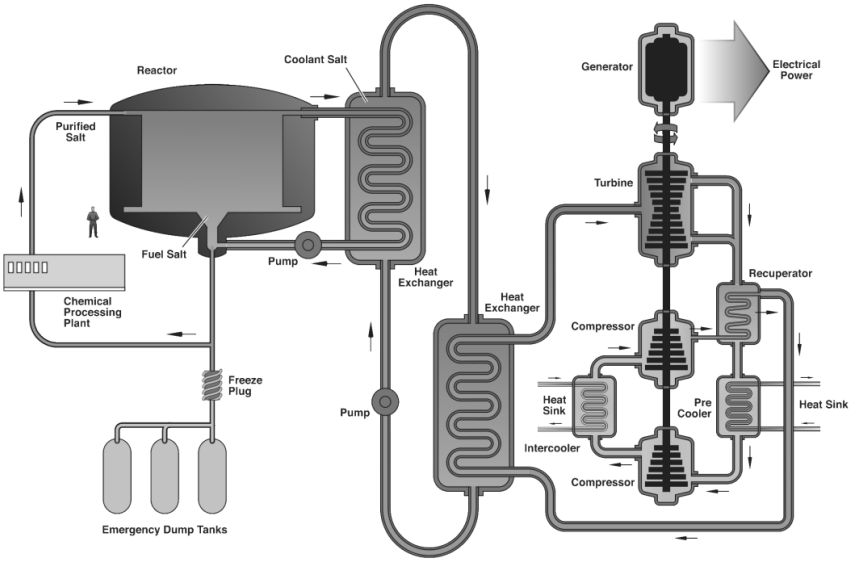

Figure 1.8. A schematic concept of the Molten Salt Fast Reactor

One big difference of the design of the MSFR with the MSRE is the absence of the moderator. The neutron spectrum becomes fast, which will make it better suitable for the transmutation of long-lived waste, while at the same time it is possible to breed ^{233}U from thorium. The breeding is done in a fertile blanket, which is located around the core of the reactor, as shown in figure 1.9 [EVOL, 2012].

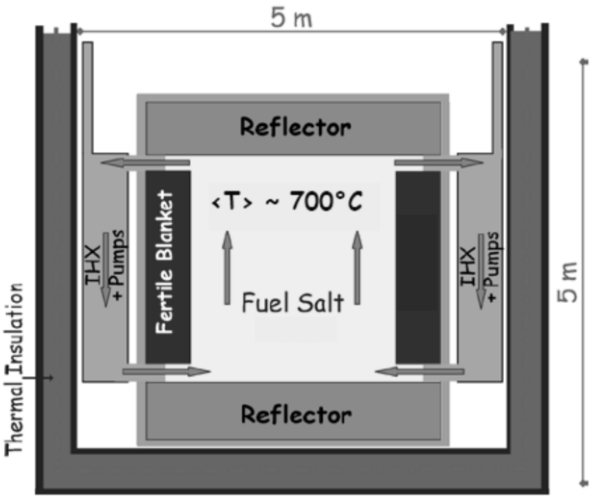

Figure 1.9. Simplified scheme of the MSFR system including the core, blanket and fuel heat exchangers.

The molten salt inside the fertile blankets is not in contact with the fuel salt and contains initially only lithium fluoride and thorium fluoride, as shown in table 1.3. The fertile blankets are used for the breeding of uranium from thorium.

Table 1.3. Composition and the properties of the salts used in a MSFR

Fuel salt	$LiF\text{-}ThF_4\text{-}^{233}UF_4$ (77.5 - 19.985 - 2.515 mole%) Or $LiF\text{-}ThF_4\text{-}(Pu\text{-}MA)F_3$ (77.5 - 16.068 - 6.432 mole%)
Fertile Blanket Salt	$LiF\text{-}ThF_4$ (77.5 - 22.5 mole%)
Properties at 700 ºC for $LiF\text{-}ThF_4$ (78-22 mol%)	
Density	4.125 g/cm^3
Specific heat capacity	1.6 $.10^3$ J/kg.ºC
Thermal conductivity	1.01 W/m.ºC
Viscosity	0.010 kg/m.s

One of the biggest advantages of the molten salt reactor is the reprocessing of the fuel during deployment. A reprocessing scheme has been established to treat used fuel by extraction of fission products. The extracted actinides are sent back into the reactor core. In this way, the wastes radiotoxicity is strongly decreased and the use of natural resource is optimized. Figure 1.10 shows a graph of the radiotoxicity of the waste of a Molten Salt Reactor (LFTR = Liquid Fluoride Thorium Reactor) compared to a normal reactor (PWR = Pressurized Water Reactor).

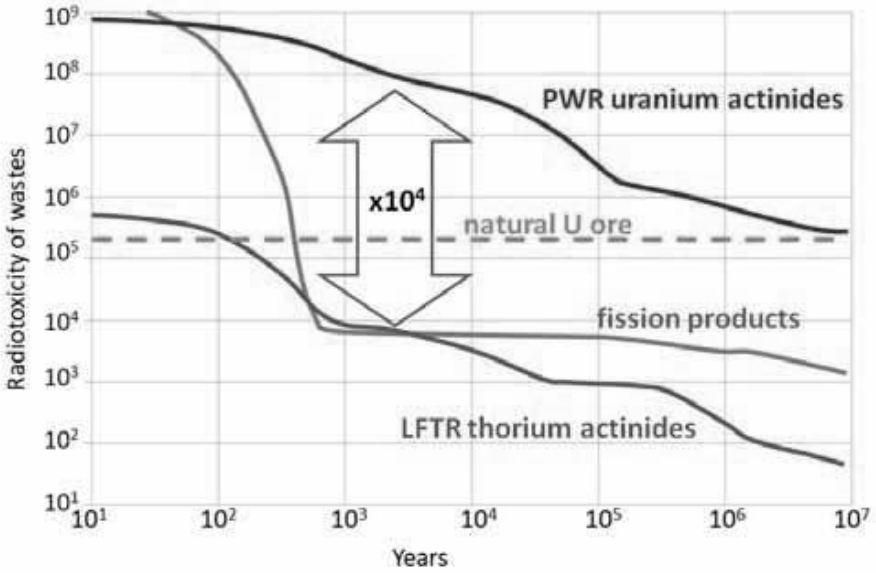

Figure 1.10. Comparison of the radiotoxicity of two different reactor designs as a function of time.

The reprocessing units can be divided into online and offline reprocessing. Online reprocessing takes place in the reactor core, where offline reprocessing takes place outside the reactor core. The next chapter will go into further detail on the offline reprocessing.

2 Offline Reprocessing Steps in a Molten Salt Fast Reactor

The liquid fuel in a molten salt reactor makes it possible to reprocess the fuel, while the reactor is still in operation. Reprocessing the salt decreases the wastes radiotoxicity, by extracting the radiotoxic actinides from the used fuel and sending the actinides back into the reactor core.

The total reprocessing scheme consists of online and offline reprocessing. The online reprocessing is done with a technique called helium bubbling. Helium bubbling is an online gaseous extraction with helium bubbles to remove gaseous fission products, Xe and Kr, and noble and semi noble metals by a flotation process. The offline reprocessing techniques are called:

- Fluorination
- Protactinium removal
- Actinide extraction
- Lanthanide extraction

The fuel can be tapped from the reactor to reprocess offline. Figure 2.1 shows a schematic drawing of the different reprocessing steps.

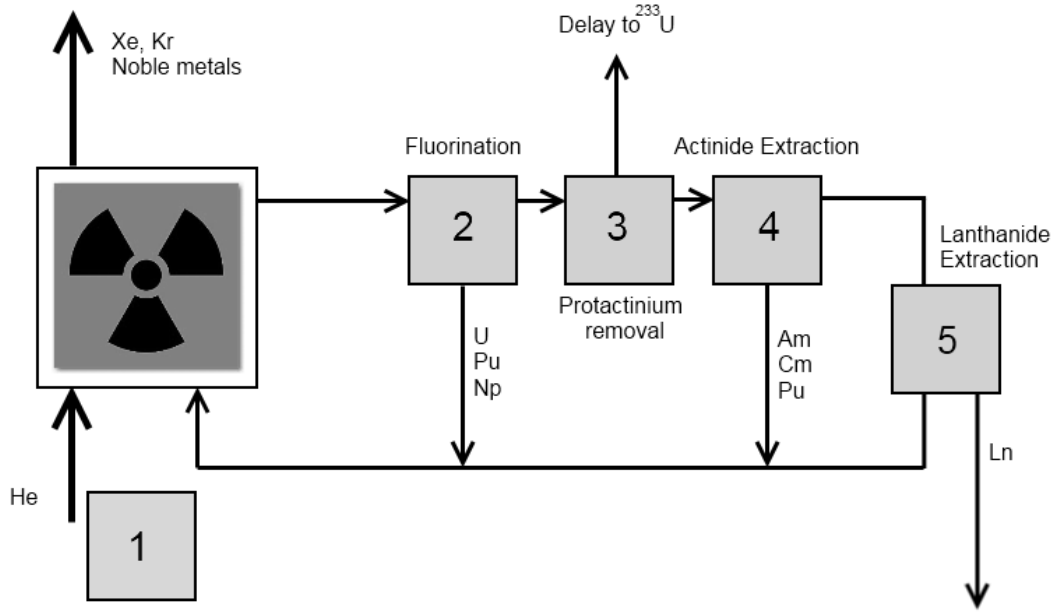

Figure 2.1. Schematic drawing of the reprocessing steps of the fuel of a molten salt reactor. With online reprocessing (1) Helium Bubbling, and offline reprocessing (2) Fluorination, (3) Protactinium Removal (4) Actinide Extraction and (5) Lanthanide Extraction.

2.1 Fluorination

The fluorination step aims at removing the elements which form volatile fluorides, in general with high oxidation states. The extraction is done with flame fluorination. The separation process is based on specific properties of uranium, plutonium and neptunium. The current research and development work in the area of Fluoride Volatility Method (FVM) is carried out at the semi-technological line called FERDA. The line is shown in figure 2.2.

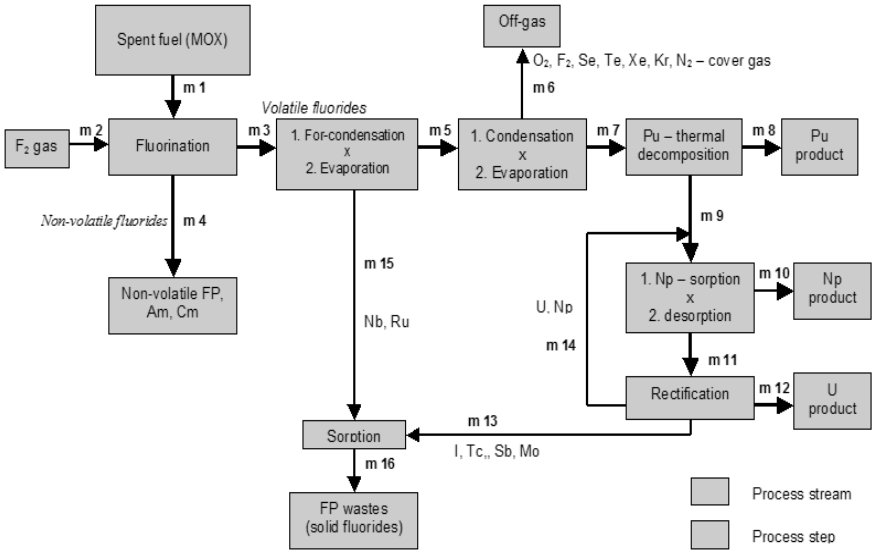

Figure 2.2. Process flow-sheet of Fluoride Volatility Method

Uranium, plutonium and neptunium form volatile hexafluorides (UF_6, PuF_6, NpF_6), where the majority of the fission products constitute non-volatile fluorides. The volatile fluorides have different boiling points, therefore it is possible to separate them by fractional distillation. Table 2.1 shows the different boiling temperatures and volatility of the different fluorides.

Table 2.1, Distribution of fluorinated spent fuel according to the volatility [Uhlíř, 2007]

Group I (highly volatile)			***Group II (volatile)***			***Group III (non-volatile)***		
Agent	m.p. (ºC)	b.p. (ºC)	Agent	m.p. (ºC)	b.p. (ºC)	Agent	m.p. (ºC)	b.p. (ºC)
Kr	-157.2	-153.4	IF_7	5	4	AmF_4	Subl.	513
CF_4	-184	-129	MoF_6	17.6	33.9	RhF_3	Subl.	600
Xe	-111.8	-108.1	**NpF_6**	**54.8**	**55.2**	SnF_4	Subl.	705
TeF_6	Subl.	-38.6	TcF_6	37.9	55.2	ZrF_4	912	918
SeF_6	Subl.	34.5	**UF_6**	**64**	**56.5**	**PuF_4**	**1037**	**927**
			PuF_6	**51.9**	**62.2**	CsF	703	1231
			IF_5	9.4	98	RbF	760	1410
			SbF_5	6	142.7	**UF_4**	**1036**	**1450**
			NbF_5	80	235	AmF_3	1427	2067
			RuF_5	101	280	CmF_3	1406	2330
			RuF_6	51	70	YF_3	1136	2230
			RhF_5	95.5	n/a	BaF_2	1353	2260
			RhF_6	70	73.5	EuF_3	1276	2280
						GdF_3	1380	2280
						CeF_4	838	Decomp.
						CeF_3	1430	2330
						PmF_3	1410	2330
						SmF_3	1306	2330
						SrF_2	1400	2460

The following reactions will take place [Delpech, 2009];

Production of gaseous F_2 and H_2:

$$2\ HF \rightarrow F_2 + H_2 \quad (2.1)$$

Fluorination of metal M:

$$MF_{(y-x)} + x/2\ F_2(g) \rightarrow MF_y(g) \quad (2.2)$$

$$\text{e.g. } UF_4 + F_2 \rightarrow UF_6 \quad (2.3)$$

Hydrogenation:

$$MF_y(g) + x/2\ H_2(g) \rightarrow MF_{(y-x)} \text{ (in the molten salt)} + x\ HF \quad (2.4)$$

$$\text{e.g. } UF_6\ (g) + H_2\ (g) \rightarrow UF_4 + 2\ HF \quad (2.5)$$

The separation of the actinides and the other fission products is done with a series of condensers, which allow separating the higher and lower boiling point components [Tulackova, 2007].

To separate the uranium, neptunium and plutonium the sorption-desorption method is used. Neptunium, plutonium and uranium fluorides can be adsorbed on a sodium fluoride bed (NaF), to separate them from the other fluoridised fission products. Neptunium and uranium can easily be desorbed with fluorine gas. Plutonium will form a thermally stable complex with the sodium fluoride traps, $PuF_4 \cdot 3NaF$. For this reason plutonium has to be separated from the other elements before entering the sodium fluoride traps. -It is possible to convert all plutonium to non-volatile PuF_4, but a part of the uranium will also be in the non-volatile form UF_4.-

Separating uranium from neptunium can be done with magnesium fluoride traps (MgF_2). UF_6 is not adsorbed on MgF_2, while neptunium is partially adsorbed. Table 2.2 shows the separation efficiencies of the different elements.

Table 2.2 Possible separation efficiencies of selected components by using fluorination. [Uhlíř, 2007]

Element	***Separation efficiency (%)***	***Method used after fluorination***
Uranium	95 - 99.9	- Adsorbed on NaF - Desorbed with F_2-gas
Plutonium	98 - 99.5	- Adsorbed on NaF - Forms complex; $PuF_4 \cdot 3NaF$
Neptunium	60 - 70	- Adsorbed on NaF - Desorbed with F_2-gas - Adsorbed on MgF_2

2.2 Protactinium Removal

It is important to remove the formed protactinium from the fertile blankets and the fuel salt, to maximize the breeding of fissile uranium (^{233}U) from thorium (^{232}Th). The reaction scheme from thorium to uranium is shown below:

$$^{232}\text{Th} + n \rightarrow {}^{233}\text{Th}\ (\beta\text{-decay}) \rightarrow {}^{233}\text{Pa}\ (\beta\text{-decay}) \rightarrow {}^{233}\text{U} \qquad (2.6)$$

When ^{232}Th captures an neutron it becomes ^{233}Th, which has a half-life of 22.2 min and undergoes β-decay to ^{233}Pa. ^{233}Pa has a half-life of 27 days and undergoes β-decay to fissile ^{233}U.

When ^{233}Pa captures another neutron it becomes ^{234}Pa, with a half-life of 1.17 min. ^{234}Pa undergoes β-decay to non-fissile ^{234}U:

$$^{233}\text{Pa} + n \rightarrow {}^{234}\text{Pa}\ (\beta\text{-decay}) \rightarrow {}^{234}\text{U} \qquad (2.7)$$

The capture cross section of protactinium is 5 to 6 times higher than the capture cross section of thorium, which makes it a big challenge to remove protactinium before it captures a new neutron, to form non-fissile uranium. Figure 2.3 gives a visual representation of the different neutron absorption cross sections. Table 2.3 gives the different cross sections in barns (10^{-24} cm^2) for thermal neutrons.

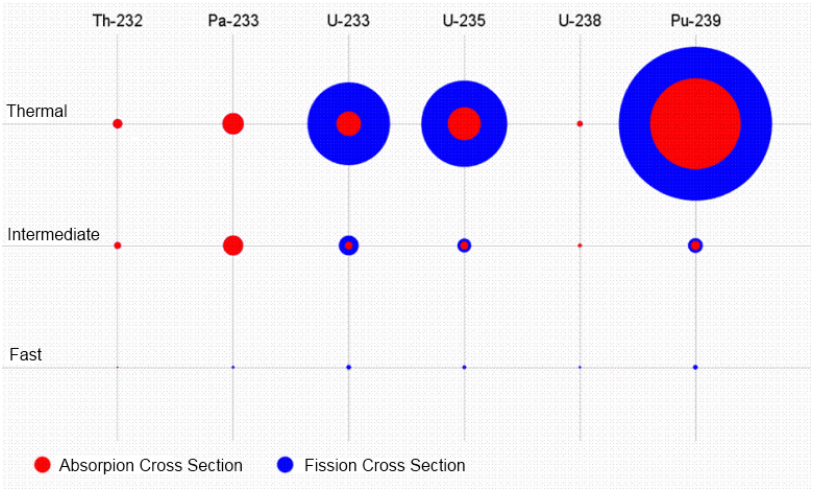

Figure 2.3. Visual representation of the neutron absorption cross sections of thorium, protactinium, uranium and plutonium for different neutron spectrums.

Table 2.3. Neutron absorption cross sections for different nuclei in a thermal neutron spectrum [Nucleonica]

Nuclide	*Capture Cross Section (barns)*	*Fission Cross Section (barns)*
^{232}Th	7.40	-
^{233}Pa	40.0	-
^{233}U	45.3	531.4
^{235}U	98.8	584.4
^{238}U	2.7	-
^{239}Pu	270.8	748.0

Protactinium can be removed by 'molten salt/liquid metal reductive extraction process' or 'metal transfer process', which is the same method used for the removal of the other present actinides. A scheme of the isolation of protactinium is shown in figure 2.4.

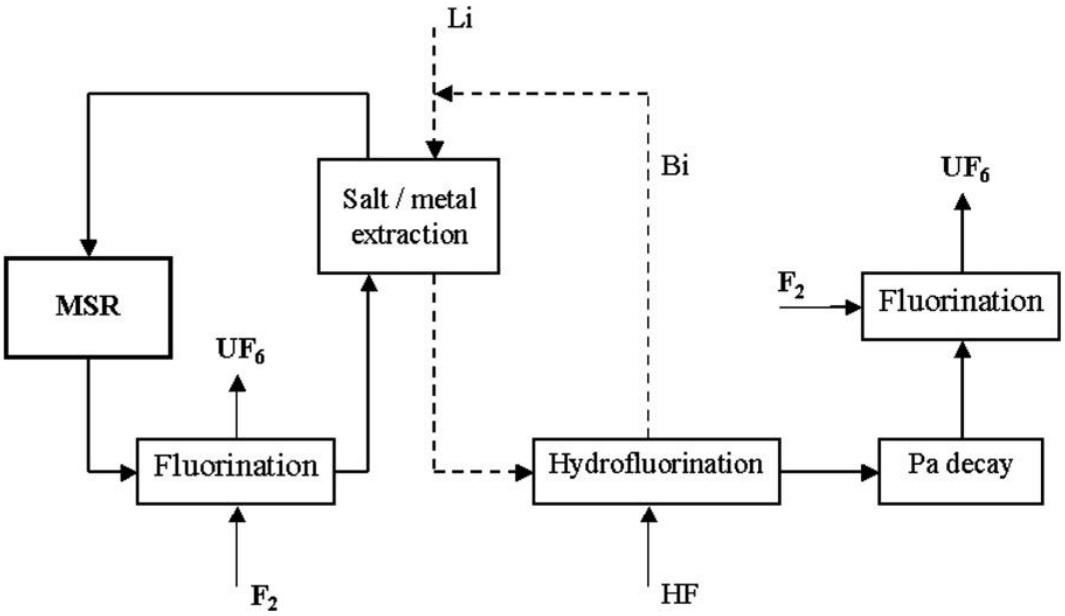

Figure 2.4, Simplified scheme of protactinium isolation from MSR fuel [Uhlíř _2, 2007].

2.3 Actinide Extraction

The remaining actinides in the fuel salt are americium, curium and the fraction of remaining neptunium and plutonium that isn't removed at the fluorination step.

2.3.1 Reductive extraction of actinides in a bismuth-thorium pool

These actinides are now extracted from the molten salt by a reductive extraction. This extraction takes place in a liquid metal solvent constituted of bismuth with metallic thorium or lithium [Delpech, 2009]. The thorium or lithium is the reductive agent, which will reduce the oxidised actinide. The thorium or lithium in the bismuth is formed to ThF_4 and LiF. The molten bismuth and molten salt are in two immiscible liquid phases. Figure 2.5 shows a schematic drawing of the reductive extraction.

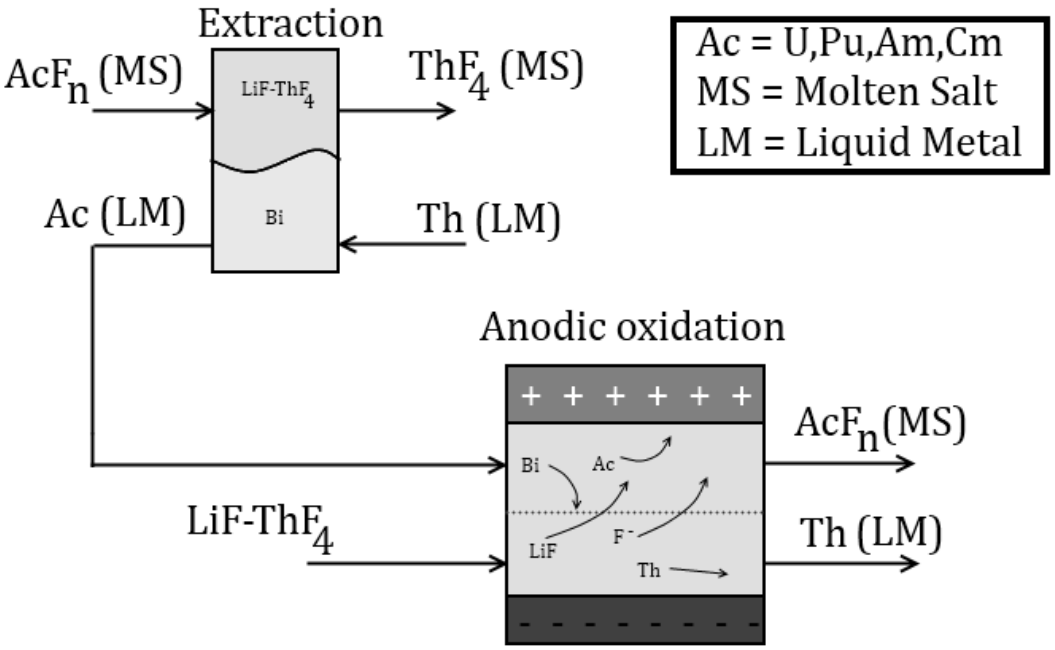

Figure 2.5. Schematic drawing of extraction and back extraction with Thorium as a reductive agent, where MS = LiF-ThF_4 and LM = molten Bismuth.

The equilibrium reactions that take place are:

$$AcF_{n\,(Salt)} + n/4\ Th_{(Bi)} \leftrightarrow Ac_{(Bi)} + n/4\ ThF_{4\,(Salt)} \quad (2.8)$$

Or

$$AcF_{n\,(Salt)} + n\ Li_{(Bi)} \leftrightarrow Ac_{(Bi)} + n\ LiF_{(salt)} \quad (2.9)$$

In general form:

$$AcF_{y\,(Salt)} + y/z\ R_{(Bi)} \leftrightarrow Ac_{(Bi)} + y/z\ RF_{z(salt)} \quad (2.10)$$

Ac = actinides
R = reductive agent

The back extraction is realized by anodic oxidation. In which the actinides oxidise and newly added ThF_4 reduces to Th. The half-reactions are:

At the cathode:

$$Ac_{(Bi)} + 3\ F^- \rightarrow AcF_3 + 3e^- \quad (2.11)$$

At the anode;

$$ThF_4 + 4e^- \rightarrow Th + 4F^- \quad (2.12)$$

With the equilibrium constant for equation (2.10):

$$K = \frac{\alpha_{Ac}\alpha_{RF_z}^{y/z}}{\alpha_{AcF_y}\alpha_R^{y/z}} = \frac{x_{Ac}\gamma_{Ac}\,x_{RF_z}^{y/z}\gamma_{RF_z}^{y/z}}{x_{AcF_y}\gamma_{AcF_y}\,x_R^{y/z}\gamma_R^{y/z}} \tag{2.13}$$

$$\alpha(i) = x(i) * \gamma(i) \tag{2.14}$$

α(i) = activity of species i
x(i) = mole fraction of species i
γ(i) = activity coefficient of species i

If the distribution coefficients are defined as:

$$D_{Ac} = \frac{x_{Ac}}{x_{AcF_y}} \tag{2.15a}$$

And

$$D_R = \frac{x_R}{x_{RF_z}} \tag{2.15b}$$

Equation (2.13) in combination with (2.15) in logarithmic form can be written as:

$$\log D_{Ac} = \frac{y}{z}\log D_R + \log K + \log\left(\frac{\gamma_{AcF_y}\gamma_R^{y/z}}{\gamma_{Ac}\gamma_{RF_z}^{y/z}}\right) \tag{2.16}$$

The importance of the activity coefficient differs in the literature:

- According to J. Finne [Finne, 2005]:

  "The γ_{MF_z} values in a fluoride molten salt are generally ranges from 1 to 10 whereas $\gamma_R^{y/z}$ and γ_M values vary between 10^{-14} and 10^{-6}. From relation (2.16) it can be seen that the outcome of the extraction depends on the values of the activity coefficients of the different compounds to be extracted both in the molten salt and in the liquid metal. Especially, the choice of the liquid metal is of primary importance."

- According to L.M. Ferris [Ferris, 1970]:

  "If the components in the bismuth phase are present at low concentration (generally less than 0.002 atom fraction); values of γ_R and γ_M should be practically constant. If in the salt phase, MF_y was either a solute present at low concentration (less than 0.002 mole fraction) or was a major component such as LiF, BeF_2 or ThF_4 whose concentration was not significantly affected by the equilibrium involved. Consequently, activity coefficients for the components of the salt phase, γ_{RX_z} and γ_{MX_y} would also be nearly constant. When the respective activity coefficients are constant, equation (2.13) reduces to:

  $$K' = \frac{x_{Ac}x_{RF_z}^{y/z}}{x_{AcF_y}x_R^{y/z}} \tag{2.17}$$

  And equation (2.16) loses the activity term:

$$\log D = \frac{y}{z} \log D_R + \log K \qquad \textit{(2.18)"}$$

2.3.2 Potential control of solvent metal

The extraction of actinides, without extracting lanthanides, is depending on the potential of the reductive agent, thorium, which is given by [Chamelot, 2007]:

$$E_{(Bi-Th)} = E^0_{ThF_4/Th} + 2.3\frac{RT}{4F} log \frac{\alpha(ThF_4)_{MS}}{\alpha(Th)_{LM}} \qquad (2.19)$$

E^0 = standard potential of redox system ThF_4/Th	(V)
R = gas constant	(J/mol.K)
T = temperature	(K)
F = constant of Faraday	(C/mol)
α = activities in Molten Salt (ThF_4) and Liquid Metal (Th)	(-)

The efficiency of extraction can be calculated with [Delpech, 2008]:

$$Eff(Ac) = \frac{1}{1 + 10^y} \qquad (2.20)$$

With,

$$y = (E_{(Bi-Th)} - E^0_{\frac{AcF_3}{Ac}}) * \left(\frac{3F}{2.3RT} - log\frac{n_{LM}}{n_{MS}} - log\frac{\gamma(AcF_3)}{\gamma(Ac)}\right) \qquad (2.21)$$

n = number of moles in the liquid metal phase (LM) and the molten salt phase (MS).

The selectivity of one actinide (Ac(1)) over another actinide (Ac(2)) is given by:

$$S\left(\frac{Ac(1)}{Ac(2)}\right) = \frac{Eff(Ac(1))}{1 - Eff(Ac(1))} * \frac{1 - Eff(Ac(2))}{Eff(Ac(2))} \qquad (2.22)$$

The amount of Thorium in the bismuth pool is adjustable, which also adjusts the potential of the bismuth pool. Adjusting the potential will adjust the efficiency and selectivity of extracting different nuclides. The redox potential for different actinides is shown in figure 2.6.

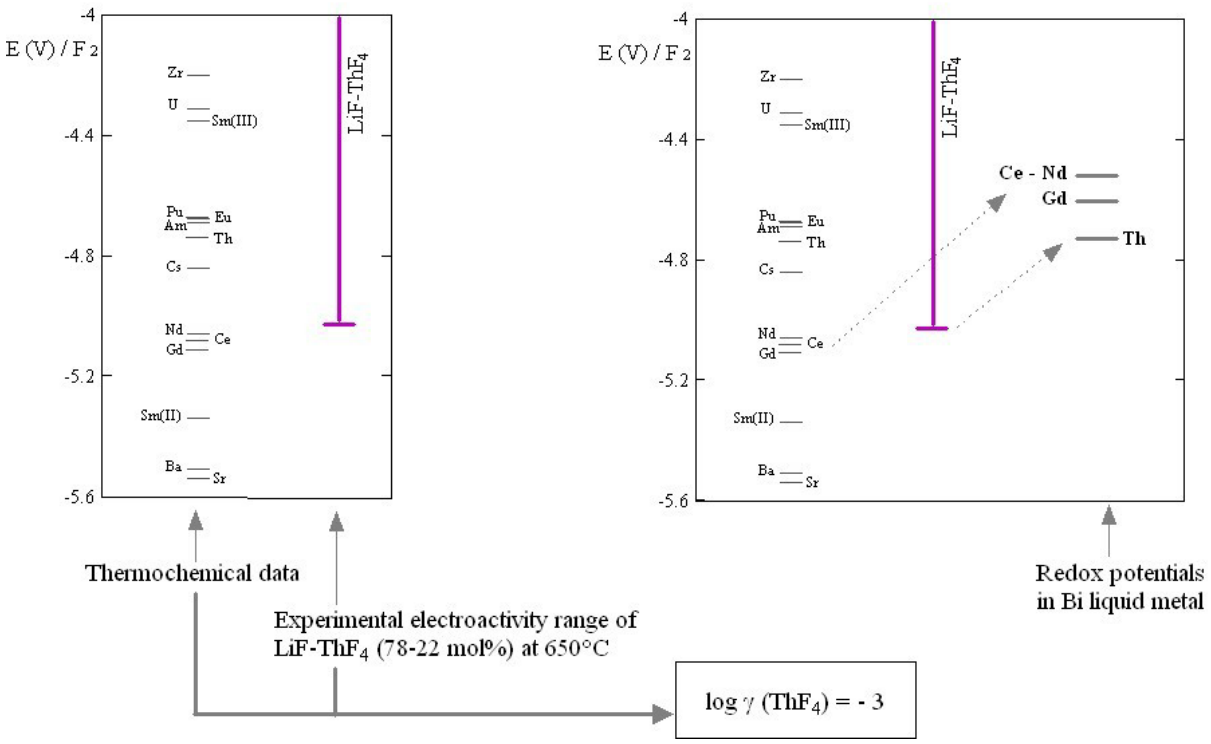

Figure 2.6. Redox potential of the different actinides and lanthanides [Delpech, 2008]

Appendix A shows an example of a selective extraction of plutonium from a sample containing plutonium and neodymium.

There are more possibilities with the reductive extraction method:

- The choice for thorium or lithium is depended on the preferred selectivity and/or efficiency of the extraction of a certain actinide. [Uhlir_2, 2007]

- The LiF–ThF4 and LiF–BeF2–ThF4 salt mixtures with comparatively high thorium concentrations (≥20–22 mol %) could not be used for effective separation of lanthanides and thorium in a system for extraction processing of fuel salts [Zagnit'ko, 2012].

- The method of reductive extraction can also be connected to the fertile blankets to extract the protactinium to give the opportunity to breed uranium. This can be a process to continuously extract newly formed protactinium.

2.4 Lanthanide Extraction

The extraction of the lanthanides is based on the same method as the extraction of the actinides. By changing the composition of the metal (bismuth) bath provides a way to control the potential, in order to selectively extract the lanthanides. See figure 2.7.

The anodic oxidation, the back-extraction of the lanthanides, will be executed with a molten salt mixture of LiCl-KCl, to form $LnCl_x$ [Auger, 2008]. The lanthanides will be oxidised with H_2O vapour to form Ln_2O_3, which will be treated as waste.

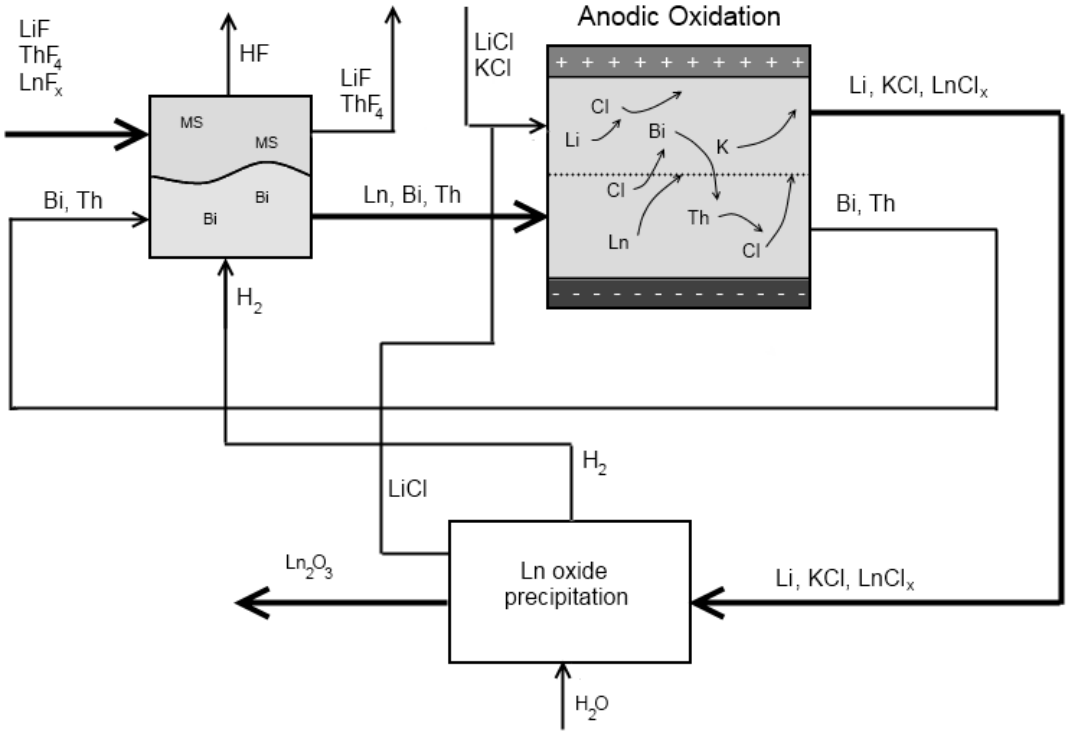

Figure 2.7. Schematic drawing of the lanthanide removal. Where Ms = molten salt ($LiF\text{-}ThF_4$).

The reaction that takes place in the bismuth pool is:

$$4/3\ LnF_{3\ (Salt)} + Th_{(Bi)} \leftrightarrow 4/3\ Ln_{(Bi)} + ThF_{4\ (Salt)} \quad (2.23)$$

The back extraction is realized by anodic oxidation. In which the lanthanides oxidise and ThF_4 reduces to Th. The half-reactions are:

At the cathode:

$$Ln_{(Bi)} + 3\ Cl^- \rightarrow LnCl_3 + 3e^- \quad (2.24)$$

$$LiCl + e^- \rightarrow Li + Cl^- \quad (2.25)$$

The lanthanide oxidation precipitation occurs according to the following reactions:

$$2\ LnCl_3 + 3\ H_2O\ (g) \leftrightarrow 6\ HCl(g) + Ln_2O_3 \quad (2.26)$$

$$Li + HCl\ (g) \leftrightarrow LiCl + ½\ H_2\ (g) \quad (2.27)$$

The formed hydrogen gas is let into the bismuth pool to reduce the ThF_4 excess. This excess occurred through the reductive extraction of the lanthanides. The reaction between hydrogen and thorium fluoride is:

$$ThF_4 + 2\ H_2 \leftrightarrow Th_{(Bi)} + 4\ HF \quad (2.28)$$

The final product of the lanthanides is Ln_2O_3 (equation 2.26), which will be treated as waste.

The lanthanides are neutron poisons, especially samarium. Figure 2.8 shows the neutron absorption cross section of samarium compared to uranium and xenon.

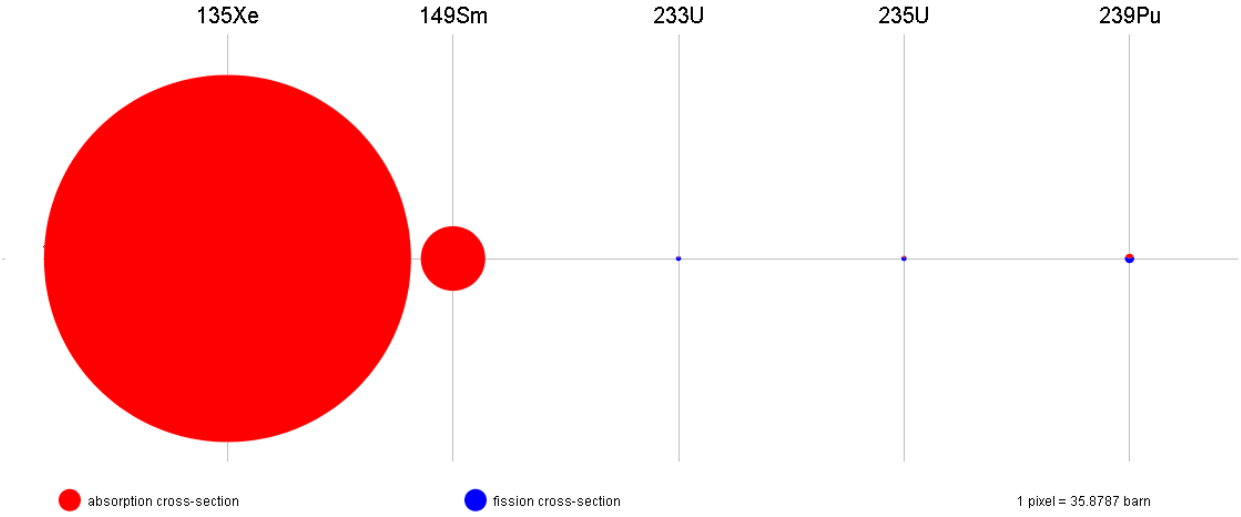

Figure 2.8. Comparison of the neutron absorption cross section of xenon, samarium, uranium and plutonium. The non-fissile samarium is one of the lanthanides with a big absorption cross-section, which makes it an important element to remove from the fuel salt.

2.5 Conclusion

Although the reprocessing scheme of the molten salt fast reactor is still in a developing stage, it shows a promising molten salt reactor concept. The individual techniques are still to be optimized. And the different steps in the offline reprocessing of the salt must finally be connected together to form a continuous process.

The insoluble fission products are the noble and semi noble metals. The online reprocessing or cleanup technique, helium bubbling, has shown promising results in extracting these metals. Helium bubbling is initially used to remove gaseous fission products, but will also remove a significant fraction of noble and semi noble metals. The precise amounts are depended on salt circulation mode, circuit geometry, flow speed, etc., and therefore difficult to predict. The next chapter will go into further detail on the removal of solid particles using the online reprocessing technique, helium bubbling.

3. Solid particles in a molten salt reactor

Most of the fission products formed in the salt in a molten salt reactor form stable fluorides that dissolve in the salt. Noble and semi-noble metals form multi-atom clusters in the molten salt and ultimately plate-out on metal surfaces, like the heat exchangers. The noble metals produce significant decay heat. If the plate-out is excessive, the decay heat from the noble metals may damage the heat exchangers via overheating should a loss of cooling occur [Forsberg, 2006].

The metals are non-wetting and insoluble relative to the salt. Metals are nonpolar, where the salt is polar. Therefore it is thought to remove the metals from the salt with a flotation process. An inert gas will be bubbled into the reactor to attach to the metals floating in the salt and to avoid that the metals plate out on the surface in the reactor. The metal particles will float with the bubbles to the surface of the liquid by the buoyancy force of the bubbles. It was found that noble and semi-noble metals were partly extracted from the salt with the online reprocessing technique of helium bubbling [Kedl, 1972].

This chapter focuses on the removal of the solid particles from the fuel salt using the helium bubbling technique.

3.1 Helium bubbling

Online reprocessing of the salt is done with helium bubbling. Helium is led into the fuel pump, which is located on top of the reactor, to extract gaseous fission products. This is a continuous process. Table 3.1 shows the elements which are volatile at a temperature of 630 ^{0}C. The most important element that will be extracted is the neutron poison xenon.

Table 3.1. List of elements with their boiling points. These elements are volatile at 630 ^{0}C and will be removed from the molten fuel salt, because of helium bubbling in the reactor

Name chemical element	*Symbol*	*Boiling-point (^{0}C)*
Helium	He	-269
Hydrogen	H	-253
Fluorine	F	-188
Oxygen	O	-183
Krypton	Kr	-153
Xenon	Xe	-108
Radon	Rn	-62
Bromine	Br	58.8
Iodine	I	184
Phosphorus	P	280
Astatine	At	337
Mercury	Hg	357
Sulfur	S	445
Arsenic	As	613

Helium bubbling extracts the gaseous fission product in 30 seconds [Merle, 2007]. Figure 3.1 shows the neutron poisons still present in the molten salt after helium bubbling, based on their cross-sections.

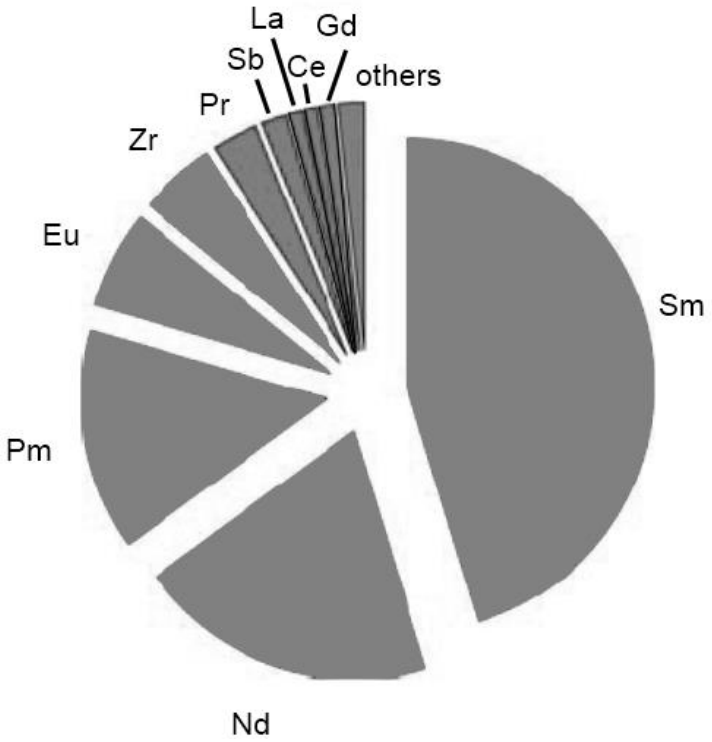

Figure 3.1. Distribution of the fission products capture rate in the core of an molten salt reactor after helium bubbling [Merle, 2005]

3.2 Materials in a flotation process

A part of the noble and semi-noble metals were found in the off-gas system of the MSRE. It is thought that the migration of the noble metals is due to a flotation process between the metals, the molten salt and helium bubbles. Flotation is a dynamic process resulting from interaction of forces acting in a bubble-particle-fluid system. The inertia of the three phases plays an important role in the flotation process. The different materials that are present in the flotation process in the molten salt reactor are noble and semi-noble metals, the molten salt and helium gas.

A new experimental method was developed during this thesis project, to get a better understanding of the different interactions in a flotation process. To avoid working with the very toxic fluorides, that are present in the molten salt, there are different liquids and fluids considered, which should have comparable properties as the materials in the molten salt reactor. The next sections are focussing on choosing the right materials for experimental simulation of a flotation process in a molten salt reactor.

3.2.1 Solids

The solids in a molten salt reactor are noble and semi-noble metals, which form nonpolar multi-atom clusters with high Palladium, Ruthenium, Rhodium and Technetium content. The densities of these

metals are given in table 3.2. The size of these clusters is unknown. The size of metals found in conventional nuclear reactors is in the order of microns.

Table 3.2. Noble and semi-noble metals found in the molten salt reactor

Name	*Symbol*	*Atomic Number*	*Density (g/cm^3)*
Molybdenum	Mo	42	10.28
Technetium	Tc*	43	11.5*
Ruthenium	Ru	44	12.45
Rhodium	Rh	45	12.41
Palladium	Pd	46	12.02

(* Tc has no stable isotope and will decay into another element, but with a halflife of 2.10^5 a)

The solids used to experimentally examine the influence in a flotation process are given in table 3.3

Table 3.3. Materials used to perform experimental research on a flotation process

Name	*Composes of*	*Density (g/cm^3)*	*Diameter (µm)*	*Polarity*
Soda lime glass	Metal Oxides	2.52	500 - 600	Polar
Polystyrene	$(C_8H_8)_n$	1.05	500 - 600	Non polar

3.2.2 Liquid

The liquid in the molten salt reactor is initially a molten salt composed of LiF-ThF_4-$^{233}UF_4$ (with 77,5 mol% LiF), which is a polar fluid. The exact characteristics for this salt are not known, but will be similar to the known salt LiF-ThF_4 (77.5 mol% LiF, 22.5 mol%ThF_4) [EVOL, 2012]. Table 3.4 shows the physicochemical properties of this salt.

Table 3.4: Physicochemical properties of LiF-ThF_4 (77.5 mol% LiF, 22.5 mol%ThF_4). Density [EVOL, 2012], dynamic viscosity [EVOL, 2012], surface tension [Yajima, 1984] .

Name	*Density @ 700 °C (g/cm^3)*	*Dynamic viscosity (Pa.s)*	*Polarity*	*Surface tension (LiF-ThF_4, 80-20 @ 722 °C) (N/m)*
Molten Salt	4.1052	0.0072	polar	0.266 ± 5.4

Uranium tetrafluoride has a higher density than thorium tetrafluoride. The fuel salt will therefore have an even higher density than is given in table 3.4.

The liquids used to experimentally examine the influence in a flotation process are given in table 3.5.

Table 3.5: Physicochemical properties of Isopar M and water.

Name	*Components*	*Density (g/cm^3)*	*Dynamic viscosity (Pa.s)*	*Polarity*	*Surface tension (N/m)*
Isopar M	C11 – C16	0.788	0.0028	Non polar	0.0257
Water	H_2O	0.998	0.001	Polar	0.0718

3.2.3 Gas

Helium gas is used to remove gaseous fission products in the molten salt reactor. Helium is an inert gas which doesn't react with the particles or the salt. In the experiment air is used as a gas.

3.3 Flotation process theory

There are some factors that play an important role to predict the interactions between bubbles and particles in a liquid. The following factors are used to predict the feasibility of a working flotation process:

- Particle settling velocity
- Force balance on a particle at the fluid interface
- Bubble rise velocity
- Bubble-particle interaction efficiency

These factors are used to compare the properties of the materials, which are considered to use in possible experimental simulation of the flotation process in a MSR.

3.3.1 Particle settling velocity

Due to gravity, particles tend to settle to the bottom of flotation cells. The velocity of the particle settling is therefore required in modeling the bubble-particle interactions and the suspension of particles in flotation.

When a particle is dropped in a liquid, there is a brief transient period as the particle experiences the acceleration due to gravity. After the transient period, the particle falls with a constant terminal velocity, which is termed the settling velocity (V_s).

The settling velocity is the velocity of the particle when the sum of de drag force (F_d) and the buoyancy force on a particle (F_{bp}) equals the gravitational force (F_g) [Nguyen, 2004a]:

$$-F_g + F_{bp} + F_d = 0 \tag{3.1}$$

With,

$$F_g = \frac{4}{3}\pi R_p^3 \rho_p g \tag{3.2a}$$

$$F_{bp} = \frac{4}{3}\pi R_p^3 \rho_l g \tag{3.2b}$$

$$F_d = \frac{1}{2}\pi R_p^2 V_s^2 \rho_l C_d \tag{3.2c}$$

Solving equation (3.1) for V_s yields:

$$V_s = \left(\frac{8R_p(\rho_p - \rho_l)g}{3C_d\rho_l}\right)^{1/2} \tag{3.3}$$

C_d is the drag coefficient, which is a function of the particle Reynolds number, which is given by:

$$Re = \frac{2R_p V_s \rho_l}{\mu} \tag{3.4}$$

$$C_d = \frac{24}{Re} \qquad for\ Re \to 0 \tag{3.5}$$

V_s can now be described as:

$$V_s = \frac{4}{9}\frac{R_p^2 g(\rho_p - \rho_l)}{\mu} \tag{3.6}$$

Figure 3.2 shows the settling velocity for different materials depending on the particle diameter.

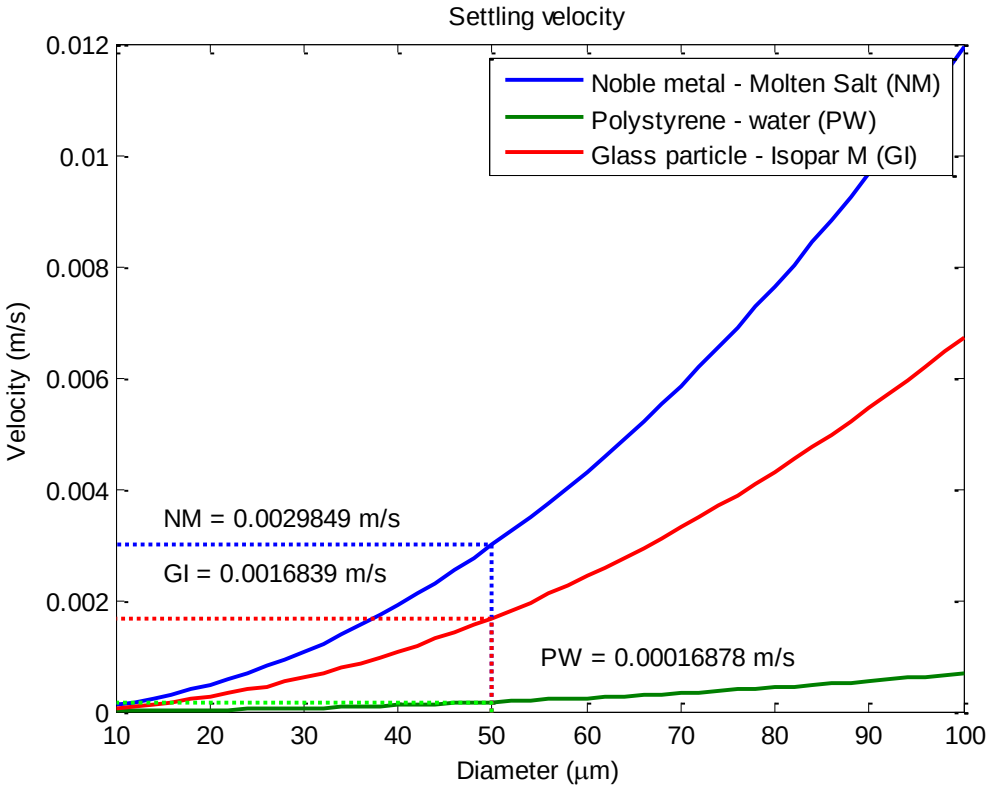

Figure 3.2, Settling velocity of a noble metal (Pd) in stationary molten salt (LiF-ThF_4, 77.5-22.5 mol%) (NM), polystyrene in water (PW) and glass particles (SiO_2) in Isopar M (hydrocarbon) (GI).

The theoretical settling velocity of polystyrene in water is low compared to the other two. The density of polystyrene is almost similar to water (1.05 g/cm^3).

3.3.2 Force balance on a particle at the fluid interface

The forces in a bubble-particle-fluid system are described by Schulze [Schulze, 1984]. The force balance for a single particle adhering to a gas bubble can be expressed as:

$$-F_g - F_s - F_a + F_b + F_h + F_c = 0 \quad (3.7)$$

With,

F_g (the gravitational force) = $\frac{4}{3}\pi R_p^3 \rho_p g$ (3.7a)

F_s (the capillary pressure in the bubble) = $\pi R_p^2 sin^2(\omega)(\frac{2\sigma_{LG}}{R_b} - 2\rho_l R_b g)$ (3.7b)

F_a (additional detaching force) = $\frac{4}{3}\pi R_p^3 \rho_p b_m$ (3.7c)

F_b (the static buoyancy force) = $\frac{1}{3}\pi R_p \rho_l g((1-\cos(\omega))^2(2+\cos(\omega)))$ (3.7d)

F_h (hydrostatic pressure) = $\pi R_p^3 \sin^2(\omega)\rho_l g z_0$ (3.7e)

F_c (the capillary force) = $2\pi R_p \sigma_{LG} \sin(\omega) \sin(\varphi_0)$ (3.7f)

A particle will stay at the gas-liquid interface, if the sum of the force balance is zero or positive. The forces on a particle are shown in figure 3.3.

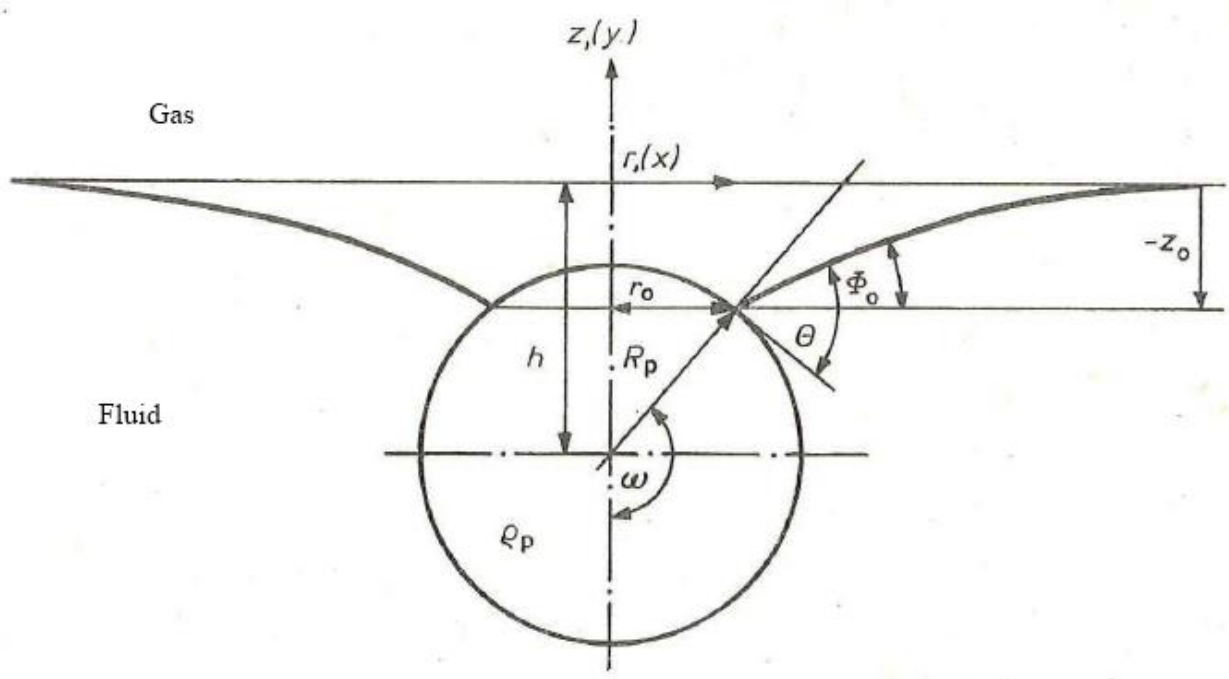

Figure 3.3. Forces on a solid particle in a gas-liquid system. [Schulze, 1983]

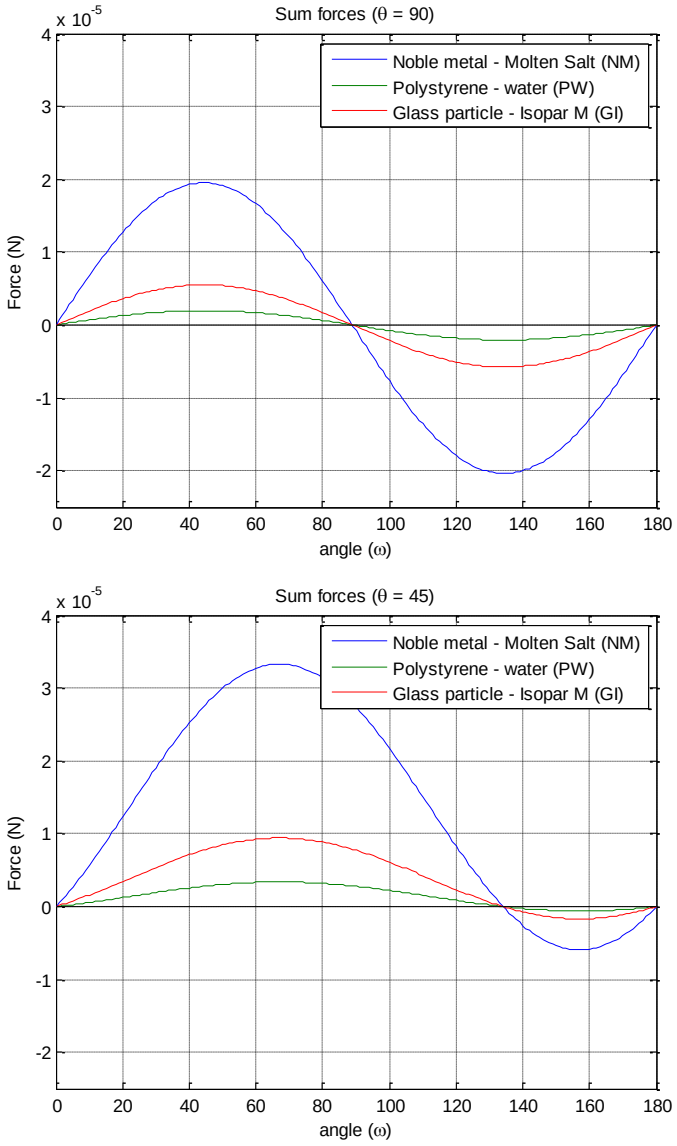

Figure 3.4. Sum of the forces on a solid particle in a gas-liquid system versus the angle ω for θ=45° and θ=90°. The diameter of the particle is 50 µm and the z-value (see figure 3.2) is 10 µm.

From figure 3.4 it can be concluded that the maximum angle ω is independent of the type of solid or fluid.

3.3.3 Bubble rise velocity

The bubble rise velocity is a function of the bubble geometry, the physical properties of the medium and the physicochemical properties of the gas-liquid interface [Nguyen, 2004b].

The bubble rise velocity of small bubbles in contaminated fluid is given by:

$$U = U_{Stokes} / \left\{ 1 + \frac{Ar/96}{(1 + 0.079 Ar^{0.749})^{0.755}} \right\} \qquad (3.8)$$

Where U_{Stokes} is the bubble terminal velocity predicted by Stokes' law and is described by:

$$U_{Stokes} = \frac{2R_b^2 g \rho_l}{9\mu} \tag{3.9}$$

The Archimedes number is defined by:

$$Ar = 8R_b^3 \frac{\rho_l^2 g}{\mu^2} \tag{3.10}$$

The terminal rise velocity for bigger bubbles is given by:

$$U = 18U_{Stokes} \left\{ \frac{4a^2 Ar^{2b-1} Mo^{0.46b}}{3k} \right\}^{\frac{1}{2-2b}} \tag{3.11}$$

Where *Mo* is the Morton number, given by:

$$Mo = \frac{g\mu^4}{\rho_l \sigma^3} \tag{3.12}$$

The constraints for a and b are given in table 3.4.

Table 3.4. Constraints for equations (3.8) and (3.11) expressed in terms of the Archimedes number and the Morton number

Equation	***Constraints***	***a***	***b***
(3.8)	$Ar \leq 12332$	-	-
(3.11)	$12332 \leq Ar \leq 3.158\ Mo^{-0.46}$	1	0
(3.11)	$3.158\ Mo^{-0.46} \leq Ar \leq 29.654\ Mo^{-0.46}$	1.14	-0.176
(3.11)	$29.654\ Mo^{-0.46} \leq Ar \leq 506.719\ Mo^{-0.46}$	1.36	-0.280
(3.11)	$506.719\ Mo^{-0.46} \leq Ar$	0.62	0

The difference in volume of a bubble will have a different rise velocity which gives a different shape bubble. The different shapes of the bubbles will have an influence on the chance of colliding with a particle. The bubble rise velocity in three different fluids is given in figure 3.5.

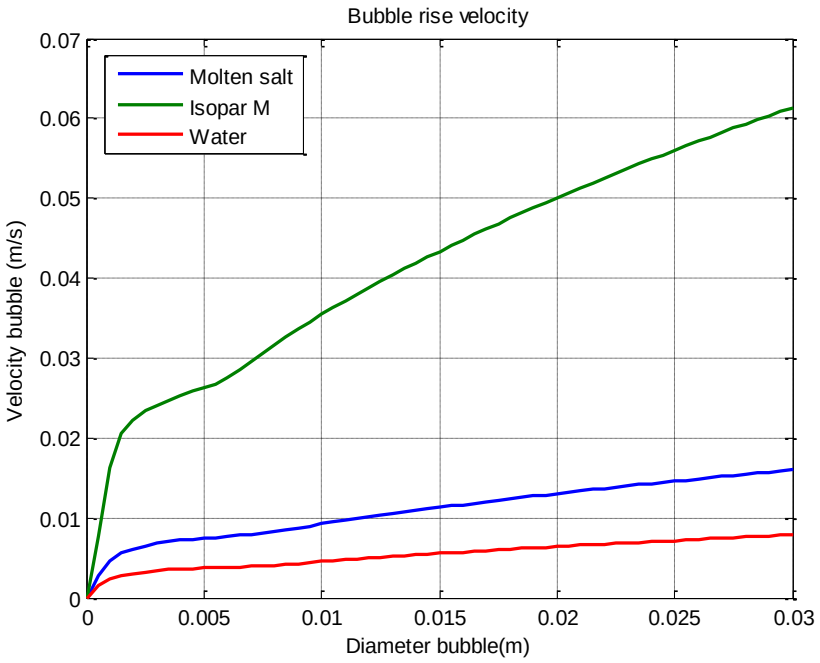

Figure 3.5. Bubble rise velocity versus the bubble diameter in a Molten Salt (77.5 mol% LiF, 22.5 mol%ThF_4), Isopar M and water.

3.3.4 Bubble-Particle Interaction Efficiency

The interaction between bubbles and particles is the key mechanism to the success of the flotation process. The three major processes that play a role in the bubble-particle interaction are:

- Bubble-particle encounter process
- Bubble-particle attachment process
- Bubble-particle detachment process

The efficiencies of these processes are best described by the rate of the particles that interact with a bubble, given in number of particles per unit of time. The general equation is:

$$E_j = \frac{N_{jr}}{Nji} \tag{3.13}$$

Where,

j = c (collision), a(attachment) or d(detachment)
r = real rate
i = ideal rate

3.4 Conclusion

The helium bubbling technique, which was initially thought to be used to extract the gaseous fission products from the molten salt reactor, can also be used to extract a significant fraction of the noble and semi noble fission products from the fuel salt in the MSR. The migration of these metals is due to a

flotation process. The factors that play a role in a flotation process are described by Schulze [Schulze, 1984] and Nguyen [Nguyen, 2004].

A new experimental method was developed during this thesis project, to verify the theories of Schulze and Nguyen and to get a better understanding of a flotation process. The development of this method includes the fabrication of a set-up and the development of a procedure to work with this set-up to gain experimental results. The next chapter will go into further detail on the experimental simulations of the flotation process.

3.5 List of common symbols

Symbol	*Description*	*Units*
a	Numerical constant	-
b	Numerical constant	-
b_m	Acceleration in the external field of flow	m/s^2
Cd	Drag coefficient	-
E_j	Bubble-particle interaction efficiency	-
F_a	Additional detaching force	$kg.m/s^2$
F_b	Static buoyancy force	$kg.m/s^2$
F_{bp}	Buoyancy force on a particle	$kg.m/s^2$
F_c	Capillary force	$kg.m/s^2$
F_d	Drag force	$kg.m/s^2$
F_g	Gravitational force	$kg.m/s^2$
F_h	Hydrostatic pressure	$kg.m/s^2$
F_s	Capillary pressure in bubble	$kg.m/s^2$
g	Gravitational force	m/s^2
k	Numerical constant (=0.95)	-
N_{jr}	Rate of interacting particles	1/s
N_{ji}	Rate of interacting particles	1/s
R_b	Bubble radius	m
R_p	Particle radius	m
V_s	Particle settling velocity	m/s
U	Terminal bubble rise velocity	m/s
U_{Stokes}	Terminal bubble rise velocity by Stokes' law	m/s
z_0	Liquid height (figure 3.3)	m
Greek symbols		
μ	Liquid viscosity	kg/m.s
ρ_l	Liquid density	kg/m^3
ρ_p	Particle density	kg/m^3
σ	Surface tension	N/m
φ	Angle at the three phase point (figure 3.3)	-
ω	Centre angle (figure 3.3)	-
Dimensionless groups		
Ar	Archimedes number	
Mo	Morton number	
Re	Reynolds number	

4 Experimental simulation of the flotation process

In the flotation process in the molten salt reactor are two variables that can be controlled; the size of the bubbles and the gas flow. The size of the bubbles can be adjusted by using different nozzles through which the gas enters the reactor. The change of the gas flow also influences the size of the bubbles.

There is a direct and an indirect method to find the influence of the bubble size and flow in the flotation process of solid particles [Nguyen, 2004c]:

- In the indirect method, a known amount of particles is added to a liquid filled column. A known volume of gas is bubbled through the liquid to encounter and attach to the particles. The attached particles will finally detach from the bubbles when they reach the liquid surface to be collected in a receiver in order to quantitatively measure the amount of attached particles. An example of such a set-up is shown in figure 4.1. Figure 4.1 shows a modified Hallimond tube, which is characterized by the slightly bended column with the concentrate receiver.

- In the direct methods, the particle trajectories passing a rising bubble are photographed or filmed. This method is used to find out how the bubbles interact with the particles and to get a better understanding how the flotation process works.

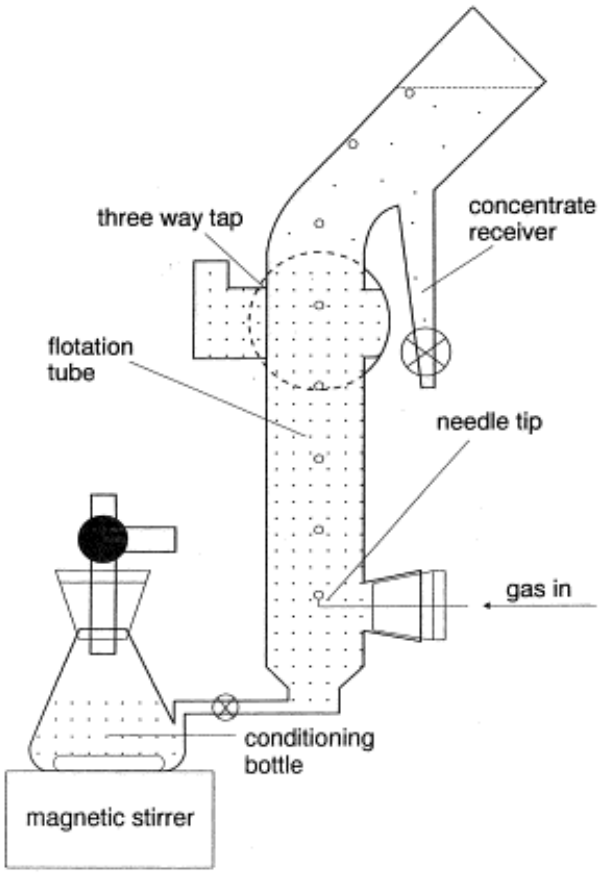

Figure 4.1. Set-up with a modified Hallimond tube.

4.1 Experimental

4.1.1 Overview of the set-up

In order to meet the conditions for both methods it was found that the set-up could be best made out of glass, because of the transparency, in order to make photos or movies from the process. Glass can also be easily adjusted in shape and size by the glass manufacturer if it doesn't meet up to the desired requirements.

The set-up is placed in a ventilated box in order to suck off the vapours from the used liquids. A schematic drawing is given in figure 4.2. A picture of the final result of the developed set-up is given in figure 4.3. The equipment is further described in section 4.2. The descriptions of the used methods are described in section 4.4.

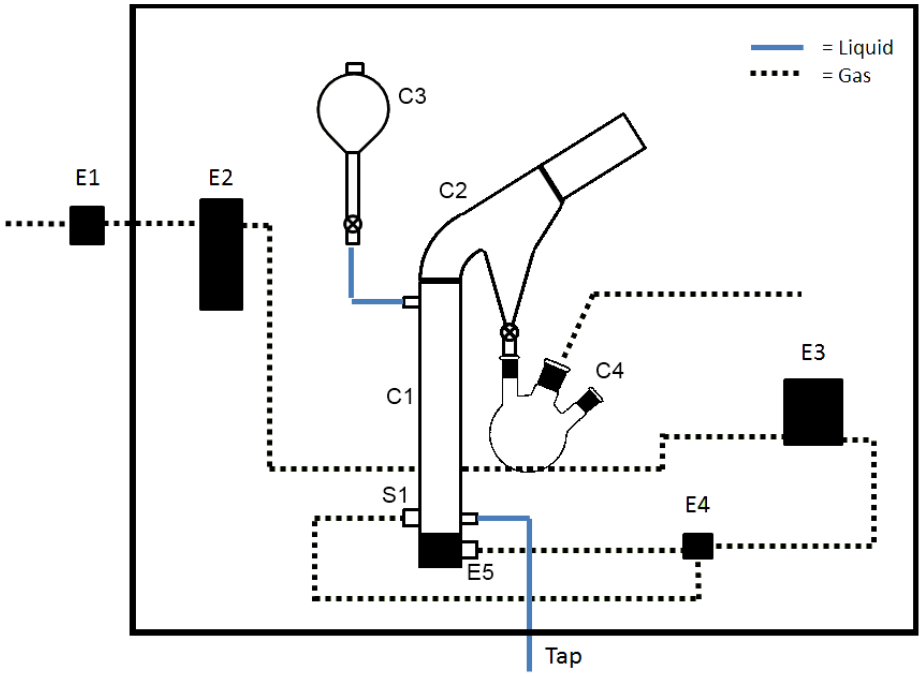

Unit	*Description*
C1	Glass column
C2	Modified Hallimond tube
C3	Glass separatory funnel
C4	Glass three-neck flask
E1	Main valve air supply
E2	Pressure controller
E3	Bronkhorst gas flow controller
E4	Three-way valve
E5	Bubble distributor
S1	Septum

Figure 4.2. Schematic overview of the set-up for a flotation experiment, the black square represents the ventilated box in which the set-up is situated.

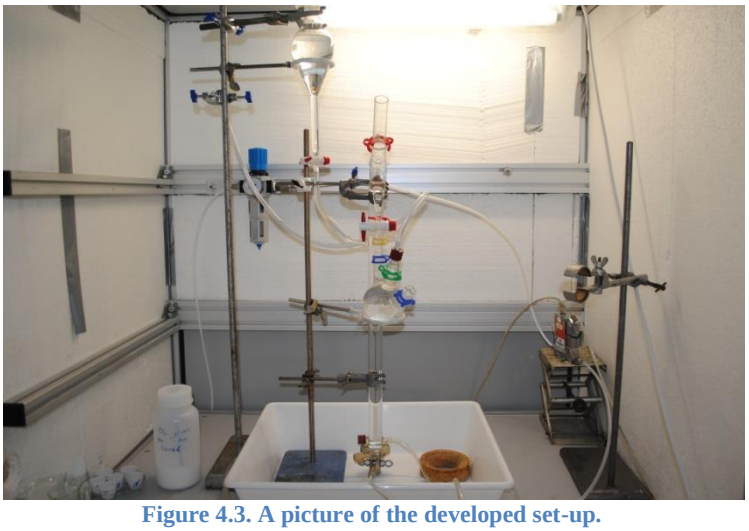

Figure 4.3. A picture of the developed set-up.

4.1.2 Description of the used equipment

Column

The basis of set-up consists of a glass column (C1) with a length of 500 mm and an inner diameter of 26 mm. and the top of the column has a NS29 ground glass joint connection. Under the top of the column is a tube connection with a diameter of 6mm. The bottom of the column has a KF25 flange connection. Above the bottom are another tube connection with a diameter of 6 mm. and a septum.

The normal joints for these columns are flanges. For this set-up the top flange is replaced by a ground glass joint to easily attach another glass piece. The tube connections are mounted on the column to be able to fill and drain the column without disassembling the whole set-up. A septum is mounted on the column to be able to let the gas enter the column through a needle. Figure 4.4 shows the top and bottom of the column, with the adjustments.

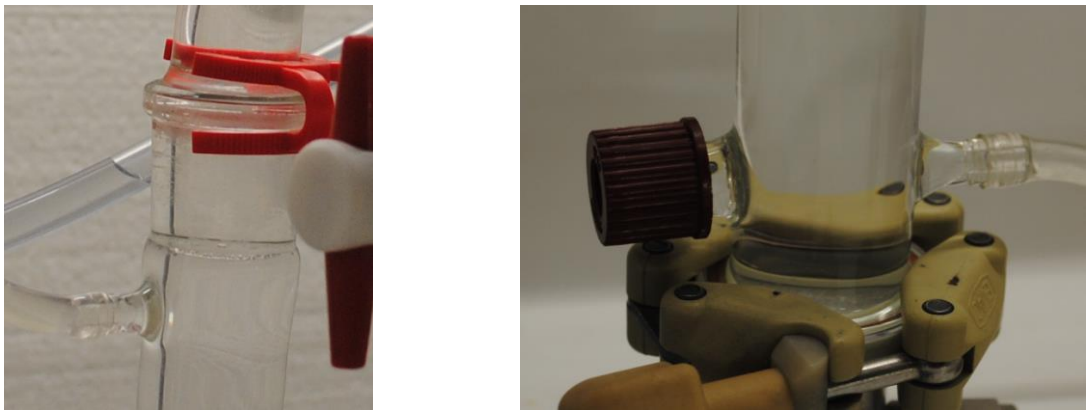

Figure 4.4. Left: The top of the column with a NS29 ground glass joint and a tube connection. Right: The bottom of the column with a septum on the left and a tube connection on the right. At the bottom is a KF 25 flange with a clamp.

Hallimond tube

On top of the column is a specially made modified Hallimond tube (C2) attached. The ends of the Hallimond tube consist of NS29 ground glass joints. The lower part of the Hallimond tube has a small valve which can be opened and closed by hand. Under the valve is a NS14.5 ground glass joint. On top of the Hallimond tube is a straight glass tube attached to the ground glass joint. The tube has a length of 100 mm and a diameter of 26 mm.

The modified Hallimond tube is the most important piece of equipment of the set-up. The tube is specially designed for this set-up in order to be able to perform a quantitative experiment. The blueprint for this tube is given in Appendix B.

The tube is constructed with a curve of 140 degrees. The choice for a curve of 140 degrees is based on earlier made Hallimond tubes. The angle of the curve is to be experimentally examined to find the optimum angle in which the rising bubbles can rise through the curve without detaching the attached particles due to a collision with the wall. On the edge of the tube is an extra reservoir to collect the particles which fall down from the liquid-gas surface. At the bottom of the reservoir is a valve to be able to close the system. Figure 4.5 shows the modified Hallimond tube.

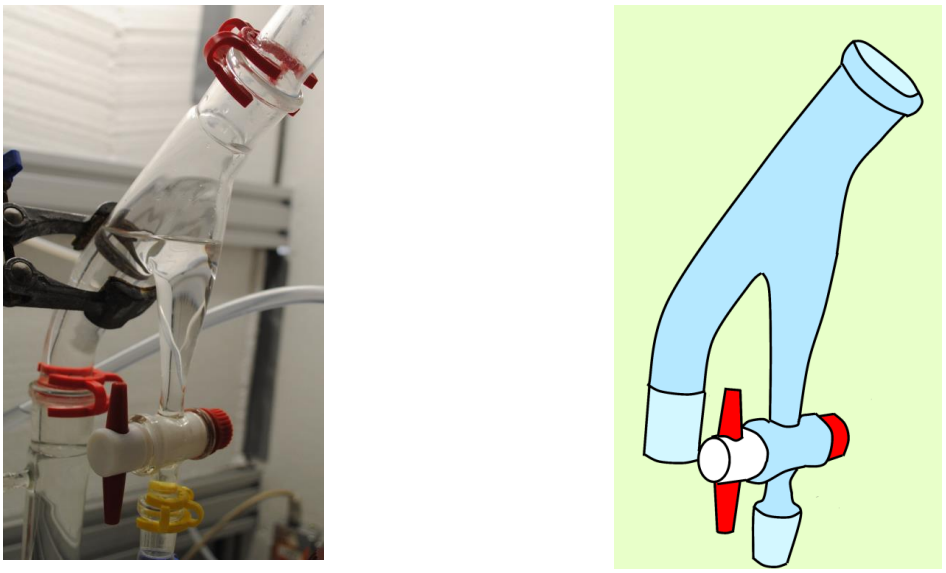

Figure 4.5. The modified Hallimond tube connected to the top of the column. The figure on the right shows a drawing of the left figure. The tube has two NS29 ground joints on the thicker parts (red clamps) and a NS14.5 ground joint (yellow clamp) under the valve. The valve can be opened and closed by hand. The valve, as shown in the picture, is open.

Three neck flask

Under the Hallimond tube is a three neck flask (C4) attached with two NS19 and one NS24 ground glass joints. The NS14.5 glass joint from the Hallimond tube is attached to the NS19 joint of the three neck flask with a transition piece NS14.5/19. The three neck flask has an NS24 tube connection on the middle neck and a plug on the second NS19 joint.

A three-neck flask belongs to the common used laboratory equipment, which makes it easy to obtain. The first neck of the flask is attached to the Hallimond tube. At the second neck a polystyrene tube is attached to function as an opening to be able to completely fill the set-up with a fluid. The opening is necessary to release the air inside an empty flask. At first it was thought to use a round flask with one neck, which was connected to the Hallimond tube, but it was impossible to completely fill the set-up with this flask. The third neck is closed with a plug. Figure 4.6 shows the three-neck flask in the set-up.

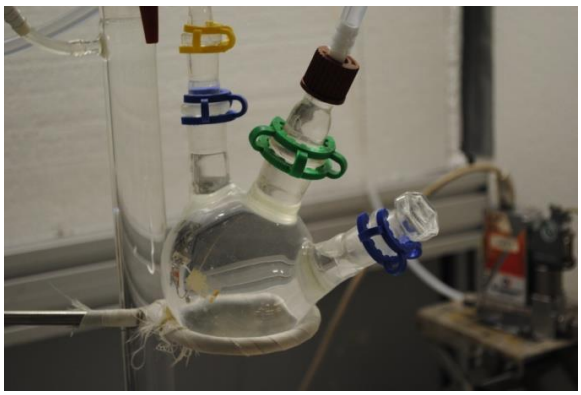

Figure 4.6. A three-neck flask is connected to the Hallimond tube. The three-neck flask is used to collect the particles that are floated to the surface by the gas flow. The first neck is connected to the Hallimond tube. A tube is connected to the second neck to release the air inside the flask during the filling of the set-up. The third neck is sealed with a plug.

Separatory funnel

The tube connection at the top of the column is attached to a separatory funnel with a polystyrene tube with a diameter of 6mm.

It was found that a separatory funnel could best be used to get all the weighted particles in the column. The separatory funnel has an outlet which is located at the bottom side. Above the output is a valve which can be handled manually. It is possible to use the weight of the particles to add them to the column, by simply opening the valve of the funnel, because the output of the funnel is at the bottom.

At first it was tried to use a small tube to add the particles in the column. But it was not possible to release all the particles in the column. A peristaltic pump was also tested to get the particles in the column. But the pump wasn't be able to pump the particles evenly around. Figure 4.7 shows the separatory funnel in the set-up.

Figure 4.7. The separatory funnel is used in the set-up to add the particles to the column. The valve can be opened and closed by hand. The funnel is filled with a liquid and the weighted particles are added to the funnel, while the valve is closed. When the particles are settled at the bottom the valve can be opened to add the particles to the column.

Bubble distributor

A sintered stainless steel distributor plate (E5) is situated between a small container and the bottom of the column. The distributor plate is a Sika R20. The small container is attached to column with a flange.

The distributor plate is used to distribute the gas flow uniformly in the column. The container will slowly be filled with the used liquid, which will enter through the pores of the distributor plate. The gas enters the bubble distributor through a small tube with an opening at the bottom. Figure 4.8 shows a picture of the distributor at the bottom of the column and a drawing of a cross section of the container through which the gas enters the column.

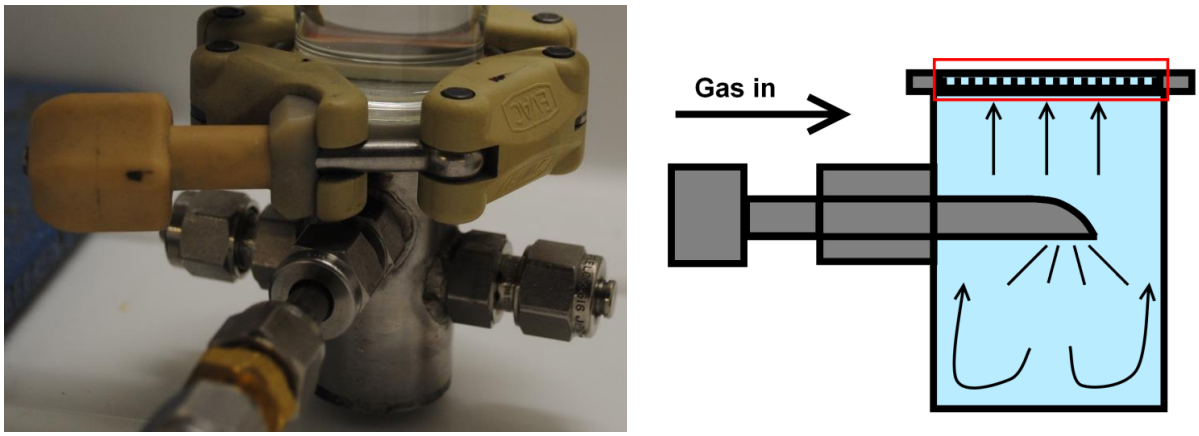

Figure 4.8. The distributor plate is situated between the column and a small container. The small container has three ends, from which two are closed and one is connected to the air supply. The container and the column are connected with a flange clamp. The figure on the right shows a cross section of the bubble distributor.

Gas supply

The used gas for this experiment is air. The air in the set-up enters the ventilated box through the main air valve. The air supply is then reduced from 6 bar gauge to 2 bar gauge by a pressure controller. The pressure controller can be adjusted by hand. A pressure meter shows the outlet pressure. The pressure controller is connected to a Bronkhorst gas flow controller. The Bronkhorst gas flow controller is directed by a computer with the following software; FlowDDE -2nd V4.67 and FlowView 7 V1.19. FlowDDE is used to connect the controller to the computer and FlowView is used to set the flow to the desired value. The output of this controller can be set between 0.00 and 1.00 l/min. It is also possible to set FlowView to a maximum amount of gas to be added to the set-up.

From the gas flow controller, the air goes through a three-way valve. This valve can be set to direct the air to the column via the bubble distributor or via a needle which can be inserted through the septum on the side of the column.

All the tubing for the gas is made out of Teflon and has a diameter of 3mm. Figure 4.9 shows the equipment used to direct the air to the column. Figure 4.10 shows the three-way valve and the bottom of the column, where the air enters the set-up through the bubble distributor or the septum.

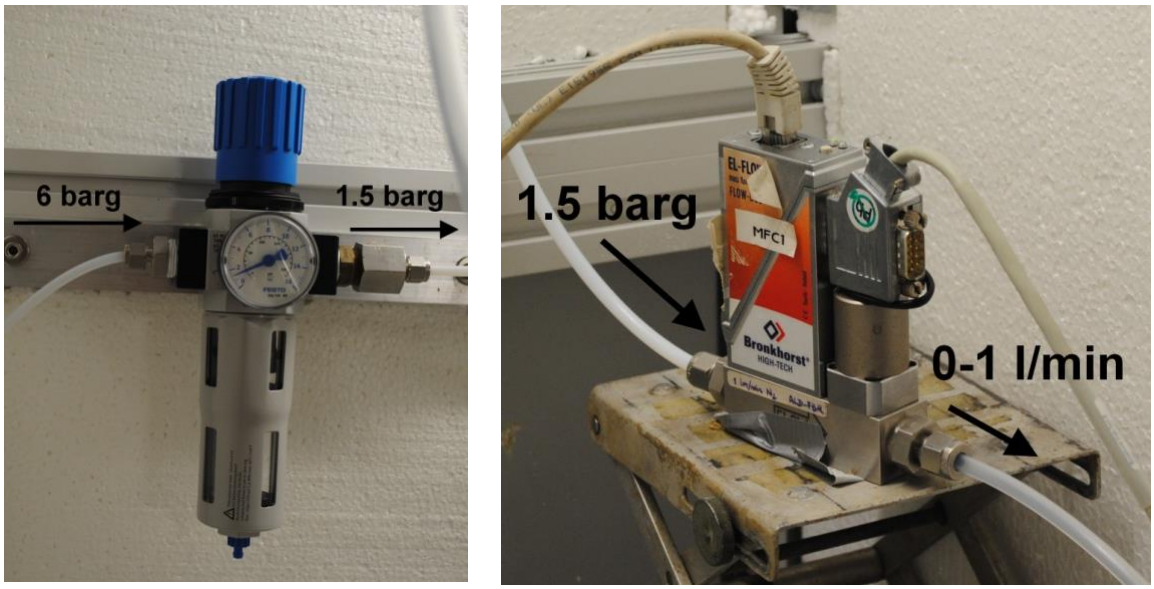

Figure 4.9. Left: Pressure controller. Right: Bronkhorst gas flow controller. The black arrows show the direction of the gas flow. The Bronkhorst gas flow controller is controlled by a computer. The cable on top of the controller is the power supply. The cable which is above the gas output is the data cable.

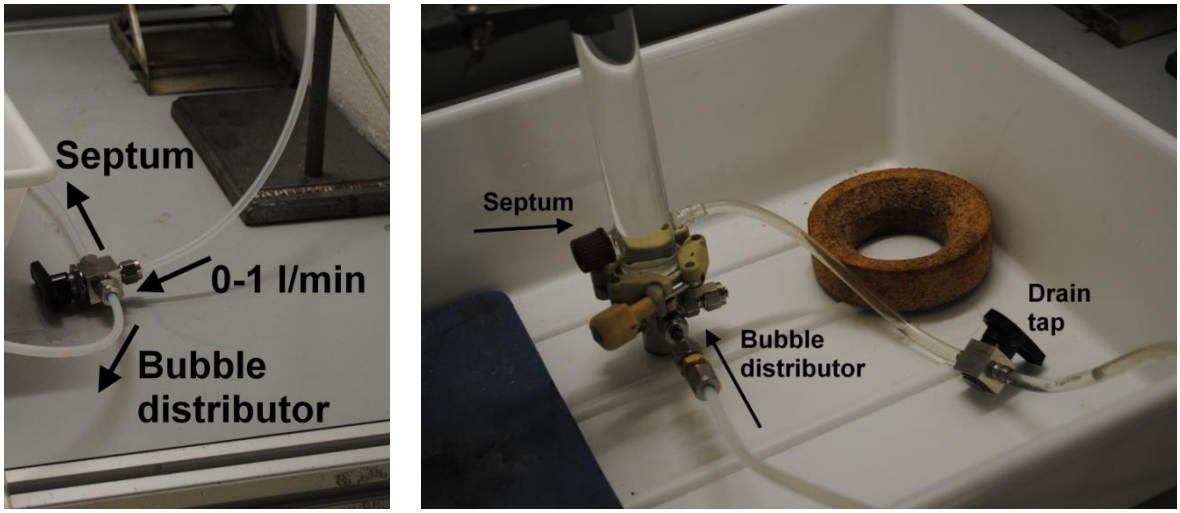

Figure 4.10. Left: Three-way valve. Right: Bottom of the column. The black arrows show the direction of the gas flow. The three-way valve distributes the air to the bubble distributor or to the septum. The right picture shows also the drain tap from the column.

Additional equipment

- An Olympus i-Speed 2 camera is used to film the process during the experiments. The camera is connected to a computer display to see the live image in order to focus the camera. The recording can be started or stopped with a second computer. This computer uses i-Speed Software Suite software.
- FlowDDE -2nd V4.67 and FlowView 7 V1.19 software
- A macro lens: TAMRON SP Di, AF 90mm 1:2.8, Macro 1:1, was used on the camera.
- Two types of distributor plates
- A sieve with pores of 75 µm is used to separate the solids from the liquid.
- Erlenmeyer flasks are used to store the liquids.
- Small ceramic containers to store the collected particles

- A stove is used to evaporate the liquid which is still on the particles. The particles will then be weighed to calculate the collected amount.

4.2 Materials

The following materials are used in this experiment:

- Solid particles (polar or non polar)
- Fluid (polar or non polar)
- Air

The properties of the different solid particles are shown in table 4.1.

Table 4.1: Properties of the different solids

Name	***Components***	***Density (g/cm^3)***	***Diameter (µm)***	***Polarity***
Soda lime glass	Metal Oxides	2.52	500	Polar
Polystyrene	$(C_8H_8)_n$	1.05	500	Non polar

The properties of the different liquids are shown in table 4.2.

Table 4.2: Properties of the different liquids

Name	***Components***	***Density (g/cm^3)***	***Dynamic viscosity (Pa.s)***	***Polarity***	***Surface tension (N/m)***
Isopar M	C11 – C16	0.788	0.0028	Non polar	0.0257
Water	H_2O	0.998	0.001	Polar	0.0718
Ethanol	C_2H_5OH	0.789	0.002	Polar	0.0224

The experiments are performed with:

- Soda lime glass particles with Isopar M, or
- Polystyrene particles with a water-ethanol mixture

4.3 Description of the experimental methods

A safety assessment sheet is needed, before starting the experiments. This sheet gives an overview of the experiment that is being done. This sheet can be found in Appendix C.

Indirect method

The set-up was filled with a water-ethanol mixture with a known composition. A batch of polystyrene particles is sieved in the range of 500 µm to 600 µm. And a weighed sample of 1.5 gram is added to the separatory funnel. After the particles were settled on the valve of the separatory funnel, the valve was opened. The particles entered the column at the top. The gas-flow controller was opened, when the particles were homogeneously dispersed in the column. The controller is set to be opened until 0.01 l. of gas is added to the column, the controller stops the flow when this amount is reached. The inlet-flow of the gas was set to 0.01, 0.02, 0.03, 0.04, 0.05 and 0.10 l/min., to compare the influence of

the flow on the attachment of the particles. This experiment is repeated with different compositions of the liquid. The first experiment is done with an ethanol-water mixture with a density of 0.912 gr/cm^3. This corresponds to a mixture of 41 vol% ethanol. The second experiment is done with a mixture of 0.883 gr/cm^3. This corresponds to a mixture of 55 vol% ethanol.

When a particle is attached to a gas bubble, it will flow with the bubble to the gas-liquid interface at the top of the modified Hallimond tube, where the particle will detach from the bubble and stay at the gas-liquid interface. The liquid-gas interface becomes saturated with particles in time. When a particle reaches the saturated liquid-gas interface it will detach from the bubble and fall into the three-neck flask. The column is slowly drained through the tap, after the flow of gas has stopped. The particles that are at the gas-liquid interface are added to the collected particles in the three-neck flask, because of the lowering of the liquid level due to the draining of the column. The three-neck flask is emptied onto the sieve to collect the particles. The collected particles are transferred to a small ceramic container, which is put into an oven for 30 minutes at 110 ºC, to evaporate the liquid on the particles. The collected particles are weighed, after they leave the oven. The weighed samples are compared to find the difference in the amount of collected particles per gas flow.

Direct method

The high-speed camera was added to the set-up to film the attachment between the particles and gas bubbles, to get a better understanding of the flotation process. Figure 4.11 shows a picture of the camera and the set-up.

Figure 4.11. A picture of a high speed camera which is filming the process. The red square indicates the display which shows the live image of the camera.

4.4 Results

The indirect method is used to find a relation between different gas flows and the yield of the particles. This method is also used to compare the yields for different densities of the liquid mixture of ethanol and water. The direct method is used to find the mechanism of a flotation process.

4.4.1 Experimental results for the indirect method

First experiment: Ethanol - H_2O mixture (41 - 59 vol%)

The column was filled with an ethanol - H_2O mixture (41 - 59 vol%) with a density of 91.2 g/cm^3. A weighted amount of polystyrene particles (500 - 600 µm) is slowly added to the top of the column (see table 5.1, Mass in). Air is added to the column, when the particles are homogeneously dispersed.

An amount of 0.010 litre of gas is added to the column. This experiment is repeated for different gas flows. The results are shown in table 4.3 and figure 4.12.

Table 4.3. The yield of the collected particles for different gas flows. The entered volume of gas is 0.01 l. The density of the liquid is 91.2 gr/cm^3.The particles have a diameter in the range of 500 - 600 µm.

Flow (l/min)	*Mass in (gr)*	*Mass out (gr)*	*Yield (%)*
0.01	1.498	1.179	78.7
0.02	1.522	1.313	86.3
0.03	1.539	1.433	93.1
0.04	1.500	1.375	91.7
0.05	1.495	1.452	97.1
0.10	1.537	1.483	96.5

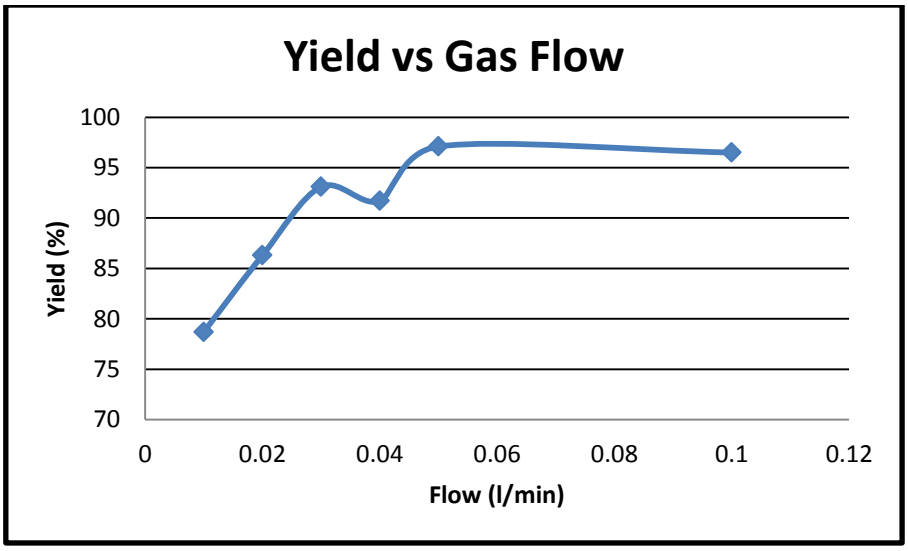

Figure 4.12. Yield of the particles for different gas flows. The entered volume of gas is 0.01 l. The density of the liquid is 91.2 gr/cm^3.The particles have a diameter in the range of 500 - 600 µm.

The difference in yield when the starting amount of particles is increased is shown in table 4.4.

Table 4.4. The yield of the collected particles for a significant difference in the initial amount of the particles. The entered volume of gas is 0.01 l. The density of the liquid is 91.2 g/cm^3.The particles have a diameter in the range of 500 - 600 µm.

Flow (l/min)	*Mass in (g)*	*Mass out (g)*	*Yield (%)*
0.01	1.498	1.179	78.7
0.01	4.515	3.977	88.1

Second experiment: Ethanol - H_2O mixture (55 - 45 vol%)

The column was filled with an ethanol - H_2O mixture (55 - 45 vol%) with a density of 88.3 g/cm^3. A weighted amount of polystyrene particles (500 - 600 µm) is slowly added to the top of the column. Air is added to the column, when the particles are homogeneously dispersed.

An amount of 0.010 litre of gas is added to the column. This experiment is repeated for different gas flows. The results are shown in table 4.5 and figure 4.13.

Table 4.5. The yield of the collected particles for different gas flows. The entered volume of gas is 0.01 l. The density of the liquid is 88.3 gr/cm^3.The particles have a diameter in the range of 500 - 600 µm.

Flow (l/min)	*Mass in (g)*	*Mass out (g)*	*Yield (%)*
0.01	1.497	1.196	79.9
0.02	1.508	1.228	81.4
0.03	1.506	1.210	80.3
0.04	1.504	1.057	70.3

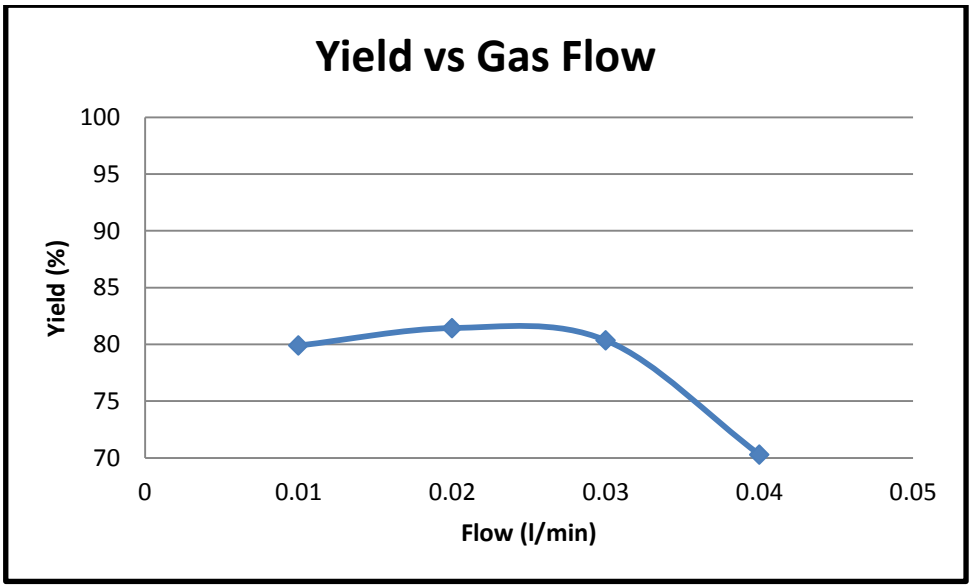

Figure 4.13. Yield of the particles for different gas flows. The entered volume of gas is 0.01 l. The density of the liquid is 91.2 gr/cm^3.The particles have a diameter in the range of 500 - 600 µm.

It was noticed that during the experiments with the current Hallimond tube, a small fraction of the extracted particles flows back into the column to either interact with another bubble or flow down to settle at the bottom of the column. There are two reasons for this behaviour. The first reason is the collision of a bubble-particle with the wall of the curve which can lead to the detachment of a particle

from a bubble. The second reason is because of an underflow at the top of the column, which allows the particles to flow over the collecting reservoir back into the column.

4.4.2 Experimental results for the direct method

4.4.2.1 Bubble size

The results for the direct method are stills from the movies made with a high speed camera. Figure 4.14 shows a series of stills of the bubbles and particles in a 55 vol% ethanol – H_2O mixture, with different gas flows.

Flow 0.01 l/min

Flow 0.02 l/min

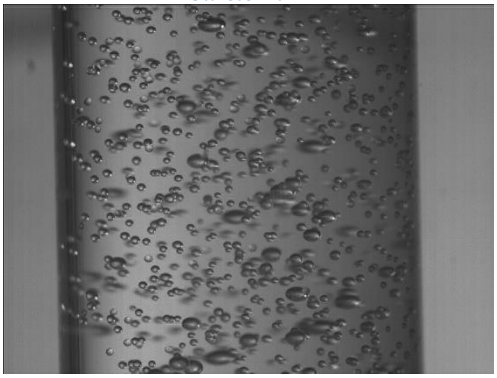

Flow 0.03 l/min

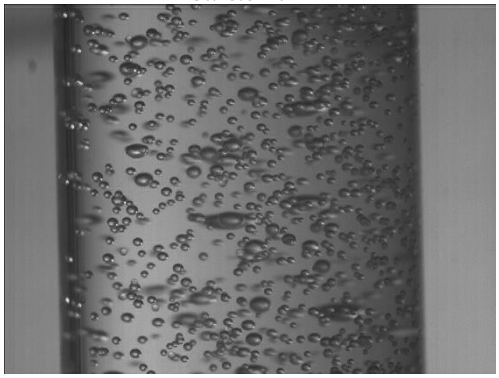

Flow 0.04 l/min

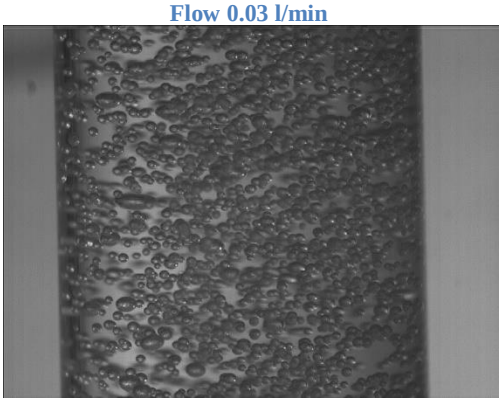

Flow 0.10 l/min

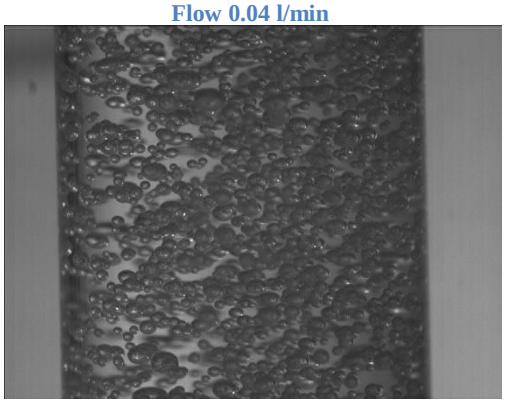

Flow 0.20 l/min

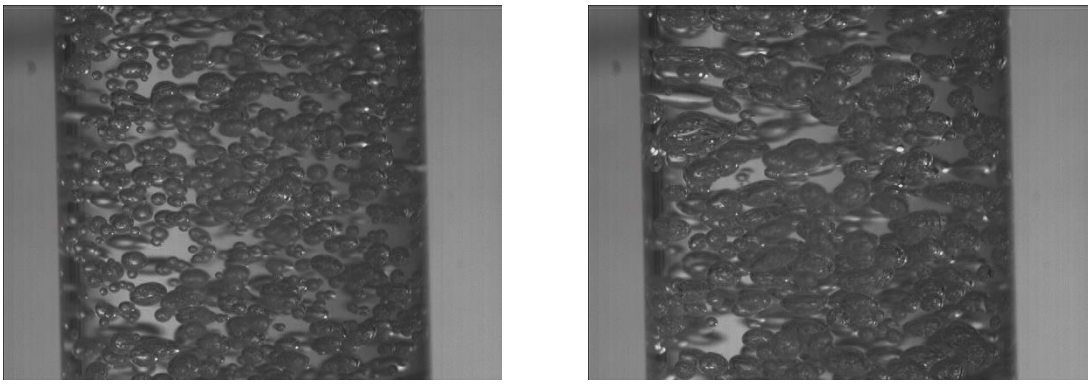

Flow 0.30 l/min Flow 0.50 l/min

Figure 4.14. A series of stills with different gas flows. The liquid is a mixture of ethanol and water (55 vol% ethanol). The gas bubbles are air. The inner diameter of the column is 26 mm. The outer diameter is 30 mm.

4.4.2.2 Speed and trajectory of an attached particle

The attachment of particles is filmed with a high speed camera. With Paint.Net and Graph Grabber V1.5.5 software it is possible to calculate the speed and follow the trajectory of the particles. Because the diameter is known it is possible to make a coordinate system.

Figure 4.15 is an example of such a system, where two different floating particles and bubbles are examined. The horizontal axes is made in paint with a straight line and copied vertically to get a line with the same length. The black square indicates the same bubbles and particles, but in another position. A description of the method to use Paint.Net to make a coordinate system is shown in appendix D.

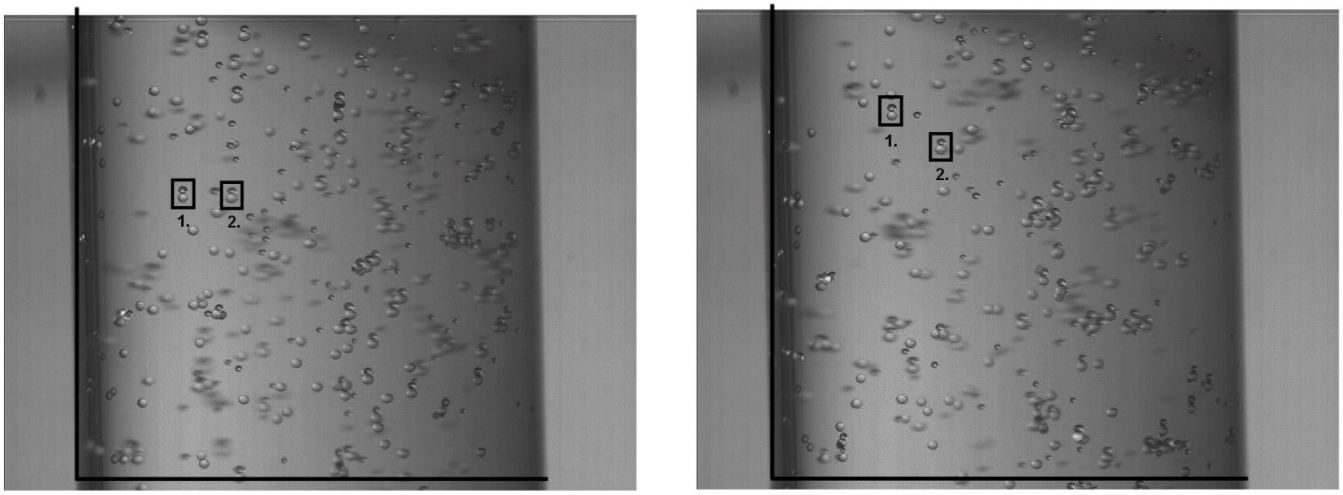

Figure 4.15. Two different particles with attached bubbles are floating upwards. A coordinate system is made with Paint.NET software. The horizontal axis is copied and pasted vertically.

The positions of the particles and bubbles can be found and stored with Graph Grabber. The method to use GraphGrabber is shown in appendix E. The coordinates are given in table 4.6 and plotted in figure 4.16.

Table 4.6. Found coordinates of floating bubbles and particles. The coordinates are found with graphgrabber

Object	*x-axis, begin*	*y-axis, begin*	*x-axis, end*	*y-axis, end*	*Difference Δx;Δy*	*Trajectory length (mm)*
Bubble 1	6.77	17.86	7.57	22.96	Δx 0.80 Δy 5.10	5.16
Particle 1	6.74	18.38	7.57	23.45	Δx 0.83 Δy 5.07	5.14
Bubble 2	9.85	17.86	10.68	20.82	Δx 0.82 Δy 2.95	3.07
Particle 2	9.91	18.33	10.70	21.28	Δx 0.79 Δy 2.96	3.06

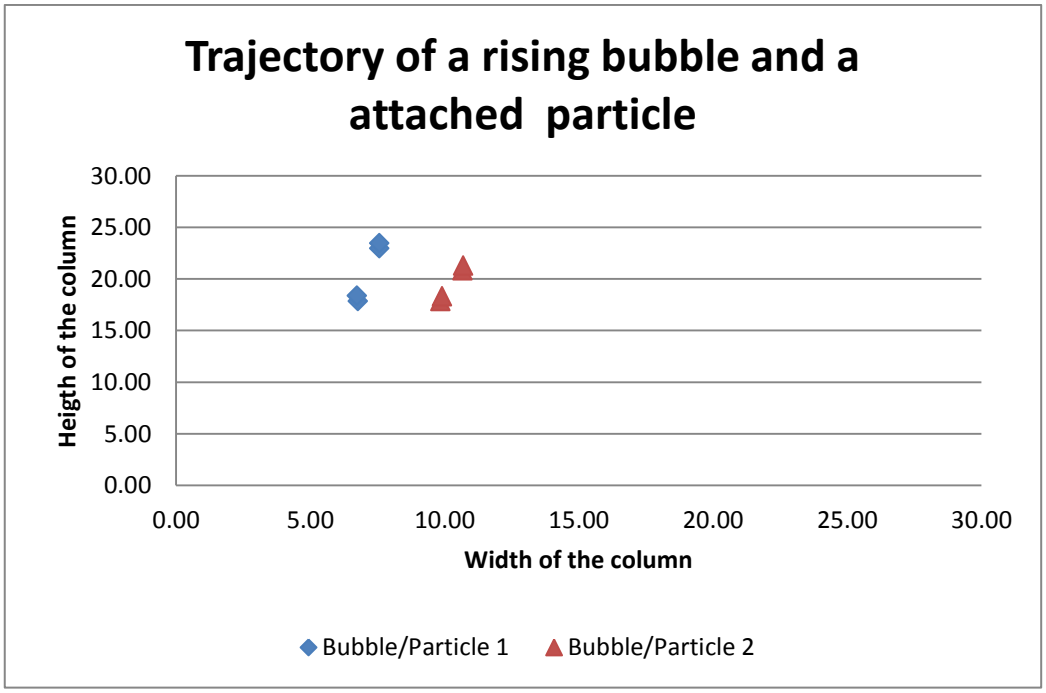

Figure 4.16. The trajectory of floating bubbles with an attached particle. The trajectory is shown in a coordinate system.

The pictures are saved under numbers. By comparing the numbers and using the frame rate of the camera it is possible to calculate the speed of the bubbles with the attached particles. The distance between the two positions is calculated and divided by the time to find the velocity of the bubble with the particle. In this example:

- The frame rate is 200 frames per second.
- The first picture is number 930 and the second picture is number 1000. The time between the two pictures is (1000-930)/200 seconds = 0.35 s.

The different speeds of the particles are shown in table 4.7.

Table 4.7. The calculated velocities of different floating particles.

Object	*Trajectory length (mm)*	*Time (s)*	*Velocity (m/s)*
Particle 1	5,14	0.35	0.0147

Particle 2	3,06	0.35	0.0088

4.4.2.3 The volume of a bubble and particle

The volumes of the bubbles and attached particles are measured with Graph Grabber V1.5.5 software the results are shown in figure 4.17. The bubbles and particles are the same as in figure 5.4.

Figure 4.17. Close-up of the bubbles and particles from figure 5.4.

The particles are considered to be spheres and the bubbles are considered to be spheroids. The volumes of the different bubbles and particles are given in table 4.8.

Table 4.8. Volumes of the different bubbles and particles from figure 4.17, with the bubble/particle ratio and the corresponding velocity of the bubble with the attached particle. The particles are considered to be spheres, the bubbles are considered to be spheroids.

Object	***Volume*** (mm^3)	***Ratio particle/bubble***	***Velocity (m/s)***
Bubble 1	0.097	1.409	0.0147
Particle 1	0.137		
Bubble 2	0.062	3.500	0.0088
Particle 2	0.218		

The velocities of the two different couples can be compared to their particle/bubble ratio. This comparison shows that the lower the ratio the higher the velocity (NB. this cannot yet be concluded to be true for every situation). The method to use Graph Grabber to measure the volumes of the bubbles and particles is described in Appendix F.

4.5 Discussion

The use of Isopar M and glass beads as materials for the experiments did not work properly, because the Isopar M reacted with the polystyrene tubing. These experiments where therefore canceled.

4.5.1 Indirect method

It followed from the first experiment that the yield increases when the gas flow increases. The yield of the extracted particles with a gas flow of 0.05 l/min (97.1 %) is nearly the same as with a gas flow of 0.10 l/min (96.5 %), which means that the yield reaches a maximum at a certain gas flow.
For the second experiment the same is true, although the yield was much lower. The maximum yield for this experiment was 81.4 % and found at a gas flow of 0.02 l/min. The main difference of the two experiments is the density difference of the liquid and the particles. The higher yields are found when the density difference is low.

The yield increases when the “mass in” is increased. It was found in the direct method that one bubble can extract multiple particles. So, when the concentration of particles increases the possibility of a bubble colliding and interacting with multiple particles increases, which is a possible explanation for this behaviour.

4.5.2 Direct method

The volume and the shape of the bubbles are depending on the gas flow. An increase of the gas flow gives an increase of the bubble volume and eventually the shape. Until a gas flow of 0.20 l/min the shape of the bubbles is mainly round. With higher gas flows the bubbles become more ellipse.

The speed of the bubble-particle is calculated by using different points of the trajectory of the bubble-particle. This method is not yet perfect, because it is based on a 2 dimensional situation, while the bubble-particles are in a 3 dimensional situation. The found velocities and trajectories are therefore not completely accurate.

The ratio of the volume of the particle and the bubble are compared with the velocity of the bubble-particle. This experiment shows that when the ratio becomes smaller, the velocity becomes higher. This cannot yet be fully concluded on the comparison of just two bubble-particles and must therefore be verified by multiple experiments on the ratio versus the velocity of bubble-particles.

5 Conclusions

The aim of this thesis was to first examine the different reprocessing steps in a Molten Salt Reactor. And secondly, the investigation of the helium bubbling technique, which can also be used to extract noble and semi-noble metals from the Molten Salt Reactor fuel.

5.1 Literature study

The first part of this thesis was to examine the reprocessing steps of the fuel salt in a Molten Salt Reactor. There are five different reprocessing steps; helium bubbling, fluorination, protactinium removal, actinide extraction and lanthanide extraction. These steps can be divided into online and offline reprocessing. Helium bubbling technique belongs to the online reprocessing group and the other reprocessing steps belong to the offline reprocessing group. The individual techniques are still to be optimized. And the different steps in the offline reprocessing of the salt must finally be connected together to form a continuous process.

The helium bubbling technique is used in the reactor to extract gaseous fission products from the fuel salt on top of the reactor core. In the literature it was found that helium bubbling technique also extracted noble and semi-noble metals from the fuel salt in this reactor. It is concluded that a flotation process takes place during the helium bubbling reprocessing technique in the Molten Salt Reactor. Therefore, there was an experimental method developed to determine the influence of the adjustable variables in a flotation process in the Molten Salt Reactor. The variables that can be adjusted are the bubble size and the gas flow.

5.2 Set-up

The second part and final goal of this thesis was to develop an experimental method to determine the influence of the bubble size and gas flow in a flotation process. A flotation process is described as an extraction of solids from a liquid with gas bubbles. The bubble size and gas flow are the variables that are adjustable in the helium bubbling technique in a Molten Salt Reactor. The development of this experimental method included the making of a new set-up with a newly fabricated piece of equipment and developing a method to work with this set-up.

The final result of the set-up is a modified version of a Hallimond tube. The set-up is made out of glass which has its advantages and disadvantages. One of the advantages of the glass parts of the set-up is the transparency. The transparency makes it possible to follow the interactions in the process. Another advantage is the possibility to easily adjust the shape of the glass. The major disadvantage of the set-up made out of glass is that it is fragile; a small part of the glass column was broken during this project when the set-up was disassembled for cleaning. Although broken parts can easily be restored, it takes a lot of time, because this has to be done by an external company. The conclusion is that the advantages are weighing up to the disadvantages.

The set-up is built to use the methods to examine a flotation process, which are described by Schulze [Schulze, 1984] and Nguyen [Nguyen, 2004]. The methods are a direct and an indirect. The indirect method is based on the extraction of a known amount of particles that are added to the set-up. The direct method is filming the direct interaction of solids with gas bubbles and is used to get a better understanding of how the process works. After testing the set-up it can be concluded that the

developed set-up is able to get good results for the direct method and promising results for the indirect method. The indirect method has to be improved by altering the modified Hallimond tube. The particles that initially were extracted by the bubbles are partially floating back into the column and will be extracted again by the newly entered bubbles, which makes it impossible to say how much bubbles are needed to extract a certain amount of particles. The set-up is therefore not yet optimised for collecting quantitative results.

5.3 Recommendations

The recommendations for future research are divided into theoretical work, set-up improvements and further research.

5.3.1 Theoretical work

To continue research on the topic of extracting noble and semi noble metals from the fuel salt of the Molten Salt Reactor, it is recommended to examine the data of more bubble-particle interactions to find a strong relation between the extractions of a particle in a known liquid by a bubble with known volume and shape in a flotation process. The comparison of extraction yields from different flotation processes should be used to predict the behaviour of the extraction of noble and semi-noble metals from the fuel salt in the Molten Salt Reactor. The data that is needed to predict the behaviour of a flotation process can be collected with the set-up described in this thesis.

5.3.2 Set-up improvements

The most important improvement for collecting quantitative results (indirect method) is adjusting the modified Hallimond tube in such a way that the particles that are being extracted by the bubbles are all collected. With the current tube, a small fraction of the extracted particles flows is not collected. There are two reasons for this behaviour:

- The collision of a bubble-particle with the wall of the curve leads to the detachment of a particle from a bubble.
- An underflow at the top of the column allows the particles to flow over the collecting reservoir back into the column.

This behaviour can be prevented by adjusting the tube. There are a couple of options to prevent this loss of extracted particles:

- The angle of the curve of the tube can be made larger to prevent the bubbles from colliding too hard into the wall.
- By placing a glass barrier in the tube the particles can be prevented to float back into the column.
- The diameter of the Hallimond tube can be widened to prevent the underflow to allow the particles to flow back into the column.

The direct method is using the diameter of the glass to determine the size of the bubbles or the length of the trajectory of the bubbles. The results don’t take into account the curvature of the glass. It has to

be examined what the deviation is of a particle or bubble in the glass per different liquid. It is therefore recommended to use an object of known dimensions into the column to find the deviation on the film.

5.3.3 Further research

The set-up can be used to collect data for a better understanding of the mechanisms of a flotation process. The methods that are described in this paper can be used to perform research on the following:

- Examine the extraction yield of the particles with different liquid densities. This can also be done with different type of liquids and particles.
- Find a relation between the extraction yield and the different gas flows in a flotation process. The yield becomes maximum at a given gas flow, increasing the gas flow will than no longer increase the yield. This knowledge can give a good inside in the optimal use of the gas supply. The relation between the gas flow and the shape of the bubbles will probably play an important role in this relation.
- Find a relation between the ratio of the volumes of the bubble-particles and the upward velocity of the bubble-particles. This relation is dependent on the force balance between the bubble and the attached particle, where the radius of the particles and bubbles play an important role.
- Investigate the influence of different distributor plates on the volume and shape of the bubbles at a given gas flow. This research can be combined with finding a relation between the density of the used liquid and the volume and shape of the bubbles at a given gas flow.
- Examine the contact angles between the bubbles and the particles and their velocities. The challenge in this research is to get very sharp close-ups of the interactions between bubbles and particles.

References

[Auger, 2008] T. Auger, G. Barreau et al., *The CNRS Research Program on the Thorium cycle and the Molten Salt Reactors*, Thorium Cycle – Molten Salt Reactors, PaceN CNRS, 2008

[Bettis, 1957] E.S. Bettis, *The Aircraft Reactor Experiment-Design and Construction*, Nuclear Science and Engineering, Volume 2, 804-825, 1957

[Chamelot, 2007] P. Chamelot, L. Massot et al., *Feasibility of the electrochemical way in molten fluorides for separating thorium and lanthanides and extracting lanthanides from the solvent*, Journal of Nuclear Materials 360, 64–74, 2007

[Delpech, 2008] S. Delpech, M. Salanne et al., *Actinides/Lanthanides separation for the thorium molten salt reactor fuel treatment*, Atalante Montpellier, 2008

[Delpech, 2009] S. Delpech, E. Merle-Lucotte et al., *Reactor physic and reprocessing scheme for innovative molten salt*, Journal of Fluorine Chemistry, Volume 130, 11-17, 2009

[EO2013, 2013] U.S. Energy Information Administration, *International Energy Outlook 2013*, DOE/EIA-0484(2013), 2013

[EVOL, 2012] EVOL Project, Molten Salt Fast Reactor, Reference configuration, 2012

[Ferris, 1970] L.M. Ferris, *Equilibrium distribution of actinide and lanthanide elements between molten fluoride salts and liquid bismuth solutions*, Journal of Inorganic and Nuclear Chemistry 32, 2019 - 2035, 1970

[Finne, 2005] J. Finne, G. Picard et al., *Molten salt/liquid metal extraction: Electrochemical determination of activity coefficients in liquid metals*, Journal of Nuclear Materials 344, 165–168, 2005

[Forsberg, 2006] C. W. Forsberg, *Molten-Salt-Reactor Technology Gaps*, Proceedings of ICAPP ’06, NV USA, paper 6295, 2006

[GIF, 2009] *Gen IV International Forum, GIF R&D Outlook for Generation IV Nuclear Energy Systems*, 2009

[Goethem, 2008] *G. Van Goethem, Generation IV reactor systems and fuel cycles (horizon 2030): technological breakthroughs in nuclear fission (int'l RD&DD)*, EC DG RTD J2, 2008

[Haubenreich, 1970] P.N. Haubenreich, J.R. Engel, *Experience with the Molten-Salt Reactor Experiment*, Nuclear Applications & Technology, Volume 8, 118-136, 1970

[Kedl, 1972] R. Kedl, The migration of fission products (noble metals) in the molten-salt reactor experiment, ORNL-TM-3884, 1972

[Merle, 2005] E. Merle-Lucotte, L. Mathieu et al., *Influence of the reprocessing on molten salt reactor behavior*, in2p3-00025413, version 1, 2005

[Merle, 2007] E. Merle-Lucotte, D. Heuer et al., *The Thorium Molten Salt Reactor: Launching the thorium cycle while losing the current fuel cycle*, Université Joseph Fourier, in2p3-00186944, version 1, 2007

[Nguyen, 2004] Anh V. Nguyen, *Colloidal science of flotation*, Surfactant Science Series Volume 118, 2004

[Nguyen, 2004a] Anh V. Nguyen, *Colloidal science of flotation*, Surfactant Science Series Volume 118, page 69 - 98, 2004

[Nguyen, 2004b] Anh V. Nguyen, *Colloidal science of flotation*, Surfactant Science Series Volume 118, page 99 - 122, 2004

[Nguyen, 2004c] Anh V. Nguyen, *Colloidal science of flotation*, Surfactant Science Series Volume 118, page 239 - 254, 2004

[Nucleonica] http://www.nucleonica.net/Applet/Decay/radioactive_decay.aspx

[Schulze, 1984] H.J Schulze, *Physico-chemical elementary processes in flotation*, Developments in Mineral Processing, 1984

[Tulackova, 2007] R. Tulackova, K. Chuchvalcova-Bimova et al., *Development of Pyrochemical Reprocessing of the Spent Nuclear Fuel and Prospects of Closed Fuel Cycle*, Atom Indonesia, Volume 33, No. 1, 2007

[Uhlíř, 2007] J. Uhlíř, M. Mareček, M. Přeček, *R&D on Fluoride Volatility Method for Reprocessing of LWR and FR Oxide-type Fuels*, Proceedings of ICAPP 2007, Paper 7253, 2007

[Uhlíř _2, 2007] Jan Uhlir, *Chemistry and technology of Molten Salt Reactors – history and perspectives*, Journal of Nuclear Materials 360, 6-11, 2007

[Yajima, 1984] K. Yajima, *Surface Tensions of LiF-ThF_4 Binary Melts and LiF-BeF_2-ThF_4 Ternary Melts*, Journal of Chemical & Engineering Data, Volume 29, page 122-124, 1984

[Zagnit'ko, 2012] A. Zagnit'ko, V. Ignat'ev, *Equilibrium Distribution of Lanthanum, Neodymium, and Thorium between Fluoride Salt Melts and Liquid Bismuth*, Russian Journal of Physical Chemistry A, Vol. 86, No. 4, 533–538, 2012

Appendix A

Reductive Extraction of Plutonium

An example of the reductive extraction is done with the selective extraction of plutonium in a sample of plutonium and neodymium, in a bismuth-pool with thorium. The selectivity equation is:

$$S\left(\frac{Pu}{Nd}\right) = \frac{Eff(Pu)}{1 - Eff(Pu)} * \frac{1 - Eff(Nd)}{Eff(Nd)} \tag{A.1}$$

An example of potential variation is given in figure 2.7. If the molar fraction of thorium in the bismuth is equal to10^{-6}, and the potential of the liquid pool is -4.28 V, then, from figure 2.7, the extraction efficiency of plutonium is of 99% and that of neodymium only 1%, according to the dotted line. For lower concentrations of thorium and higher potential values, the extraction efficiency of plutonium decreases. In this case, the extraction of large fraction of plutonium would require several extraction stages [Delpech, 2009].

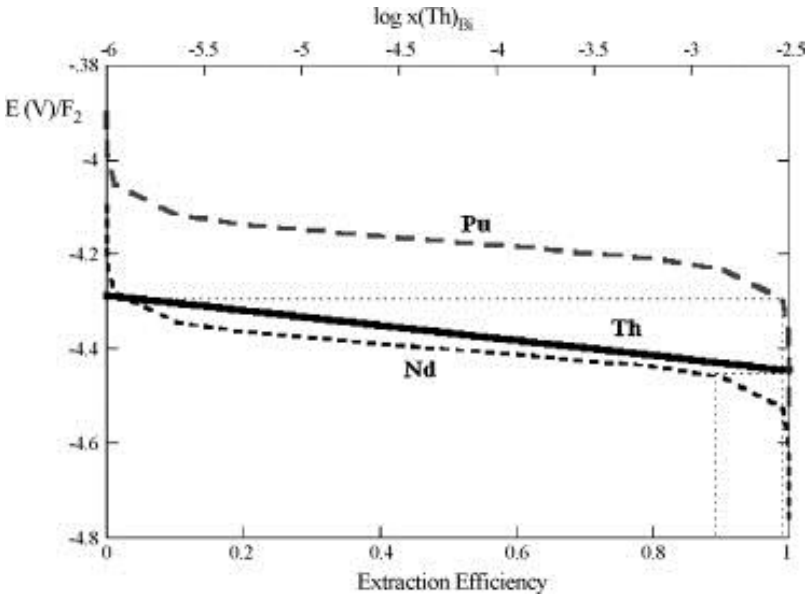

Figure A.1. Extraction efficiencies of a Bi-Th pool as a function of different potentials and thorium concentration in a bismuth bath. The dotted line shows a potential of -4.28 V, which corresponds with an extraction efficiency of plutonium of nearly 100% and for neodymium around 1%.

Appendix B

Blueprint of the modified Hallimond tube

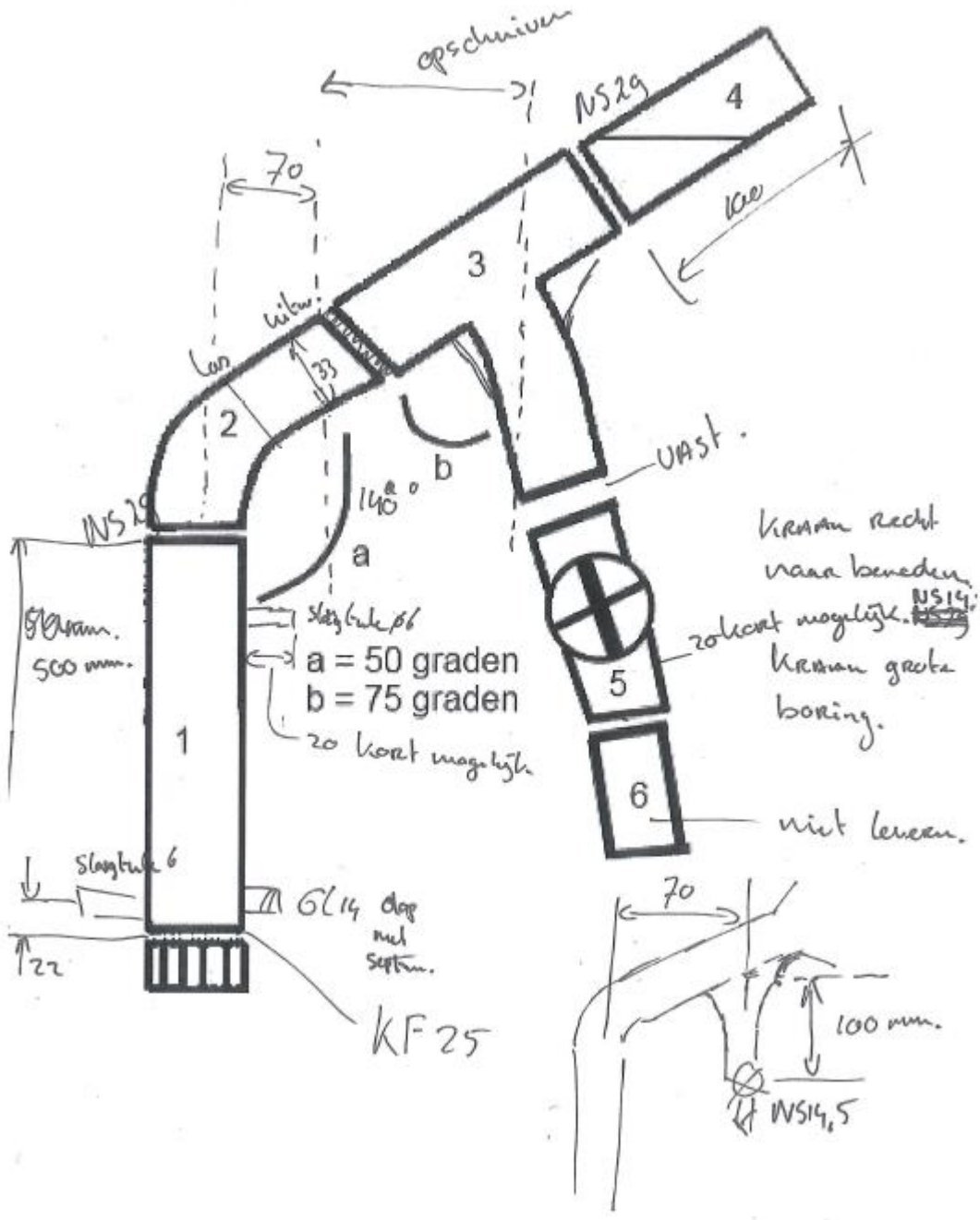

Figure B.1. Blueprint of the modified Hallimond tube

Appendix C

Safety Assessment Sheet for the floatation set-up

TU Delft Delft University of Technology	Delft University of Technology Faculty of Applied Sciences Chemical Engineering department	**ChemE**
"Safety Assessment Sheet"		

Author:	Name	*Dirkjan Journée*	Phone	0654694766
	room nr.	PF Rekenruimte		
Area Supervisor:	Name	Ruud van Ommen	Phone	015 27 82133
	room nr.	PF 02.[030]		
Experiment identification	Name	Flotation tube with gas controller		
	location	PF Ground floor	Ventilated box	

Description of experiment (including chemical equation, conditions and aim)

The goal of the experiments is to determine the effect of bubble size and flow in a three-phase flotation process. A liquid (water/ethanol mixture) filled column is used with homogeneously dispersed polystyrene particles (2 gram, 425 - 450 micron) and air is added as a gas.
The inlet gas flow is 6 barg, which is reduced by a pressure controller to 2 barg. A mass flow controller controls the gas flow into column (max 1l/min).

Temperature (°C)	Room temperature	Pressure (bar)	Gas inlet (max): 6 barg Column: Atmospheric

Labels that apply (chemicals and warning signs)

								
☐	☐	X	☐	☐	X	☐	X	☐
								
☐	☐	☐	☐	☐	☐	☐	☐	☐

Emergency shut-down procedure

Close main valve of air supply and pressure controller

Remarks

List of equipment:
1 glass column
1 Sintered stainless steel Distributor plate
1 modified Hallimond tube
1 three-neck flask
1 Separatory funnel
1 Bronkhorst gas flow controller
1 pressure controller
1 Three-way valve
1 computer
3 glass flasks
The setup is situated inside a ventilated box.

Assembly:
-Connect Bronkhorst gas flow controller to computer and close valve with the computer
-Connect gas inlet, pressure controller and gas flow controller
-Fix distributor plate
-Connect gas flow controller and distributor plate
-Fix column
-Fix Hallimond tube
-Fix three-neck flask
-Insert liquid
-Insert particles

Operation:
- Open main air valve and pressure controller
- Open valve of Bronkhorst gas flow controller

Shutdown, disassembly and cleaning
-Close main air valve and pressure controller
-Close valve of gas Bronkhorst gas flow controller
-Drain column via tap
-Detach three-neck flask
-Clean glasswork with water

Disposal of waste:
- Evaporate ethanol in open air inside the ventilated box
- Drain water through sink
- Dispose polystyrene beads as household waste

Approval of the area supervisor

Name		Date:	Valid through:
Signature			

Chemicals (including gasses) and biological materials

Chemical name and related pictograms	Give H&P statements	Storage category
Polystyrene	None given	**Solid**
Glass Beads	None given	**Solid**
 Ethanol	H225: Highly Flammable liquid and vapour H302: Harmful if swallowed H371: May cause damage to organs P210: Keep away from heat/sparks/open flames/hot surfaces. No smoking. P260: Do not breathe dust/fume/gas/mist/vapours/spray.	**Liquid**
 Isopar M	H304: May be fatal if swallowed and enters airways. EUH066: Repeated exposure may cause skin dryness or cracking P210: Keep away from heat/sparks/open flames/hot surfaces. No smoking. P301 + P310: If swallowed: Immediately call a POISON CENTER or doctor/physician. P331: Do NOT induce vomiting. P370 + P378: In case of fire: Use water mist, foam, dry chemical product of CO2 for extinction. P403 + P235: Store in a well-ventilated place. Keep cool. P405: Store locked up. P501: Dispose of contents/container according to local rules.	**Liquid**

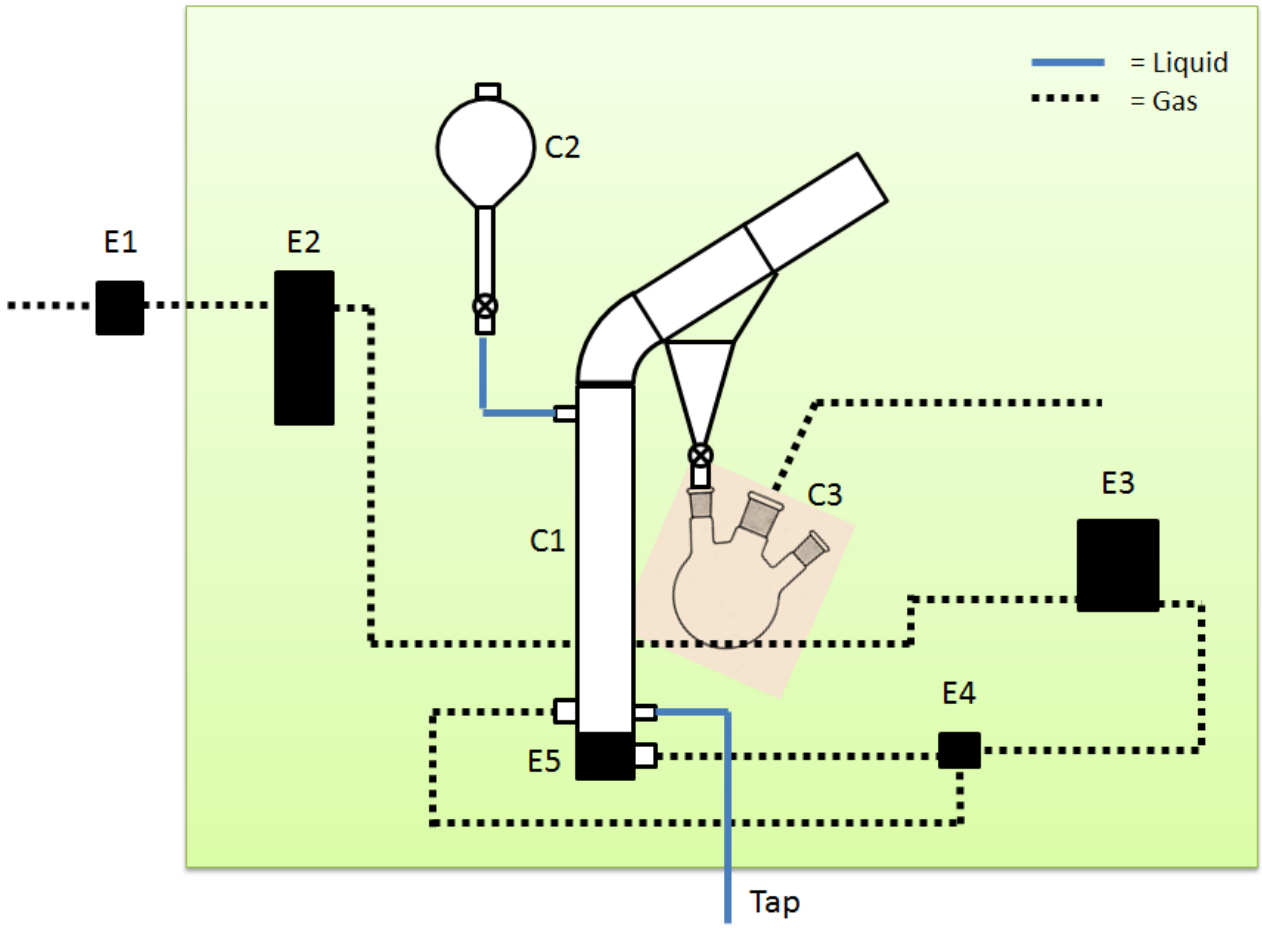

E1	Main valve air supply
E2	Pressure controller
E3	Bronkhorst gas flow controller
E4	Three-way valve
E5	Bubble distributor
C1	Glass column with modified Hallimond tube
C2	Separatory funnel
C3	Three-neck flask

Appendix D

Making a coordinate system in Paint.Net

Creating a coordinate system on an image is done with the following steps:

- open the image with Paint.Net (free software)
- make sure that there is free space around the image, e.g. the blank page in Paint.Net must be bigger than the size of the image, in order to be able to work around the image [1]
- if the recorded image isn't perpendicular, it is optional to tilt the image into the right angle
- add an extra layer to the image [2], the new layer is needed to be able to draw over the image instead of on the image
- Make a straight horizontal line on this layer (button A), which will be the x-axis [3]
- Select the line and copy this line onto a third layer drag the line and rotate it (right mouse button + Shift) into a vertical position, using the arrow keys makes it possible to move the line with small steps into the right position, this will be the y-axis [4]

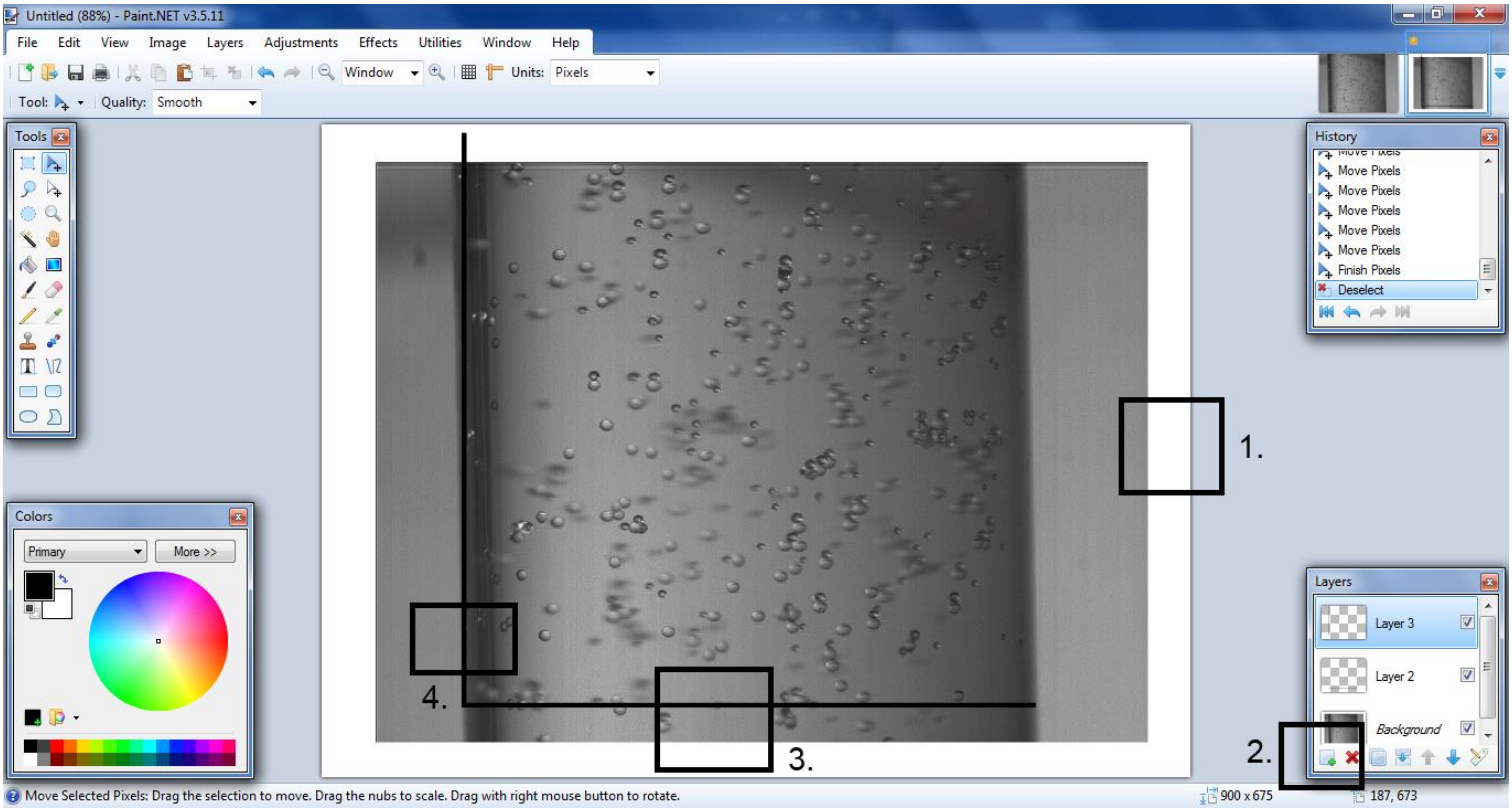

Figure D.1. An overview of the steps to make a coordinate system on an image.

Appendix E

Determine the positions of the bubbles and particles on an image using Graph Grabber

Graph Grabber V1.5.5 is a free tool which is developed by Quintessa and can be found on:

- http://www.quintessa.org/software/downloads-and-demos/graph-grabber.html

GraphGrabber is a tool that enables you to retrieve data from graphs in the form of image files. It does this by allowing users to import their graph image into the software and then to trace over it using various graphing tools to capture the data.

The steps to collect the positions of certain particles or bubbles are:

- open an image (with known axis)
- use the buttons [1] to set the image in the right position
- use the next buttons [2] to set the axis
- with the button add data series, you can collect data from the image
- the data is exported from the file menu

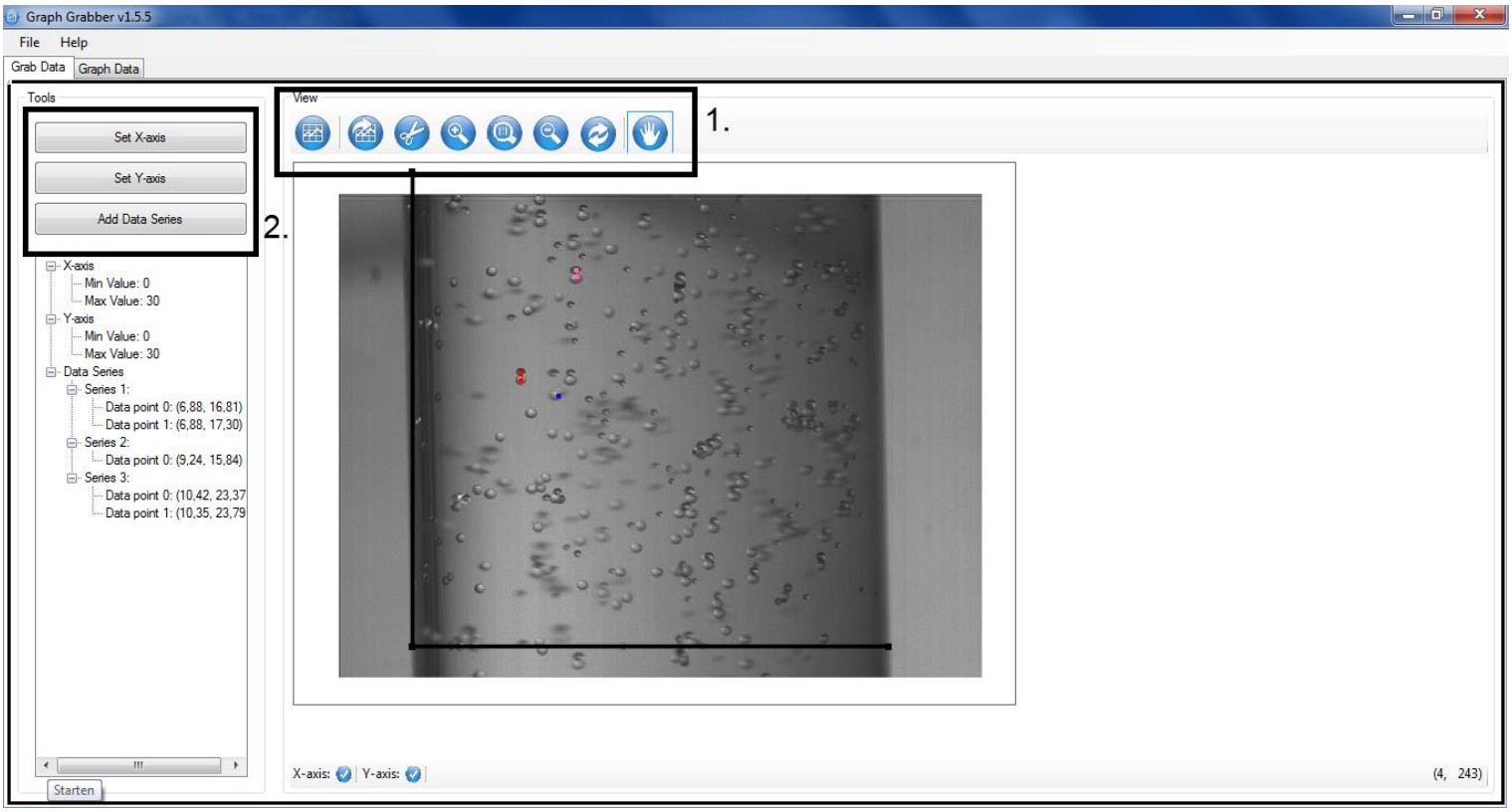

Figure E.1. Screenshot of GraphGrabber

Appendix F

Determine the volume of the particles and bubbles using Graph Grabber

The volumes are calculated as follows:

- Particle = $\frac{1}{6} * \pi * d^3$
  - Where, d is the diameter of the particle
- Spheroid = $\frac{1}{6} * \pi * (2a)^2 * 2c$
  - Where;

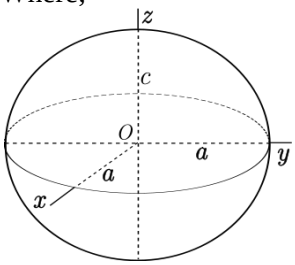

The different lengths are collected with GraphGrabber as shown in figure F.1.

Figure F.1. Using GraphGrabber to find the dimensions of the bubbles and particles

Nomenclature

Symbol	*Description*	*Dimension*
a	Numerical constant	-
b	Numerical constant	-
b_m	Acceleration in the external field of flow	m/s²
Cd	Drag coefficient	-
D	Distribution coefficient	-
E^0	Standard potential of redox system	V
E_j	Bubble-particle interaction efficiency	-
Eff	Extraction efficiency with actinide extraction	-
F	Faraday constant	C/mol
g	Gravitational force	m/s²
k	Numerical constant (=0.95)	-
K	Equilibrium constant	-
N_{jr}	Rate of interacting particles	1/s
N_{ji}	Rate of interacting particles	1/s
R	Gas constant	J/mol.K
R_b	Bubble radius	m
R_p	Particle radius	m
S	Selectivity at actinide extraction	-
T	Temperature	K
V_s	Particle settling velocity	m/s
U	Terminal bubble rise velocity	m/s
U_{Stokes}	Terminal bubble rise velocity by Stokes' law	m/s
z_0	Liquid height (figure 3.3)	m
Greek symbols		
α(i)	Activity of species i	-
γ(i)	Activity coefficient of species i	-
μ	Liquid viscosity	kg/m.s
ρ_l	Liquid density	kg/m³
ρ_p	Particle density	kg/m³
σ	Surface tension	N/m
φ	Angle at the three phase point (figure 3.3)	-
χ(i)	Mole fraction of species i	-
ω	Centre angle (figure 3.3)	-
Dimensionless groups		
Ar	Archimedes number	$8R_b^3\frac{\rho_l^2 g}{\mu^2}$
Mo	Morton number	$\frac{g\mu^4}{\rho_l\sigma^3}$
Re	Reynolds number	$\frac{2R_pV_s\rho_l}{\mu}$
Acronyms		
Ac	Actinides	
ARE	Aircraft Reactor Experiment	
CNRS	Centre National de la Recherche Scientifique	

EVOL	Evaluation and Viability of Liquid Fuel Fast Reactor Systems
FVM	Fluoride Volatility Method
GIF	Generation IV International Forum
INOPRO	Innovation-Optimization-Process
LFTR	Liquid Fluoride Thorium Reactor
LM	Liquid Metal
LMFBR	Liquid Metal Fast-Breeder Reactor
MOX	Mixed oxide
MS	Molten Salt
MSR	Molten Salt Reactor
MSFR	Molten Salt Fast Reactor
MSRE	Molten Salt Reactor Experiment
NEPA	Nuclear Energy for the Propulsion of Aircraft
OECD	Organization for Economic Cooperation and Development
ORNL	Oak Ridge National Laboratory
PWR	Pressurized Water Reactor
R	Reductive agent
UOX	Uranium dioxide